[Digitare il testo]

European Territorial Cooperation Programme
Greece - Italy
2007-2013

INVESTING IN OUR FUTURE

Co-funded by the European Union (ERDF)
and by National Funds of Greece & Italy

Efficient Irrigation Management Tools for Agricultural Cultivations and Urban Landscapes

IRMA

WP6

Specialized research actions

www.irrigation-management.eu

Deliverable 6.3.3. Report regarding valuation of satellite images for evapotranspiration estimation

European Territorial Cooperation Programmes (ETCP)

GREECE-ITALY 2007-2013

www.greece-italy.eu

Efficient Irrigation Management Tools for Agricultural Cultivations and Urban Landscapes (IRMA)

www.irrigation-management.eu

IRMA partners

Educational Institution of Epirus (LP, Lead Partner, TEIEP)

http://www.teiep.gr, http://research.teiep.gr

http://fla.teiep.gr (Hydroconcept R&D team)

Olympiaki S.A., Development Enterprise of sterGreece (P2, AEPDE)

http://www.aepde.gr

P3, INEA and from 2015: P7, CREA

Istituto Nazionale di Economia Agraria (INEA)

Consiglio per la ricerca in agricoltura e l'analisi dell'economia agraria (CREA)

http://www.inea.it, http://sito.entecra.it/

Consiglio Nazionale delle Ricerche - Istituto di Scienze delle Produzioni Alimentari (P4, ISPA-CNR)

http://www.ispa.cnr.it/

Regione di Puglia (P5, ROP)

http://www.regione.puglia.it

Decentralised Administration of Epirus–Western Macedonia (P6, ROEDM)

http://www.apdhp-dm.gov.gr

Publication info

WP6: Specialized research actions

Deliverable 6.3.3. Report regarding valuation of satellite images for evapotranspiration estimation

The work that is presented in this ebook has been co-financed by EU / ERDF (75%) and national funds of Greece and Italy (25%) in the framework of the European Territorial Cooperation Programme (ETCP) GREECE-ITALY 2007-2013 (www.greece-italy.eu): IRMA project (www.irrigation-management.eu), subsidy contract no: I3.11.06.

Deliverable 6.3.3. Report regarding valuation of satellite images for evapotranspiration estimation

WP6: Specialized research actions

Involved partners:

CREA (P7), ex INEA (P3)

Team:

Dr. Vanino Silvia Dr. Falanga Bolognesi Salvatore Dr. Pulighe Giuseppe	Dr. Nino Pasquale Dr. De Michele Carlo Dr. Nizza Giuliana

Place and time:

Rome, 2015

European Territorial Cooperation Programme Greece - Italy 2007-2013

INVESTING IN OUR FUTURE
Co-funded by the European Union (ERDF) and by National Funds of Greece & Italy

European Territorial Cooperation Programmes (ETCP)
GREECE-ITALY 2007-2013
www.greece-italy.eu

Efficient Irrigation Management Tools for Agricultural Cultivations and Urban Landscapes (IRMA)

www.irrigation-management.eu

Contents

Introduction 9
1. Remote Sensing for Determining crop water requirements from satellite optical data: methodological background 10
2. Study area 12
3. Resources 14
3.1 LICOR LAI-2000 Plant Canopy Analyzer 14
3.2 Satellite images 14
3.3 Metereological data 15
3.4 Ancillary data 18
4. Methodology 19
4.1 Selection and purchase of image 20
4.1.1 Basics 20
4.2 Pre-processing of images 21
4.2.1 Georeferencing 21
4.2.2 Image radiometric correction 21
4.2.3 Atmospheric correction 21
4.2.4 Mosaicking 22
4.2.5 Vegetation Indices 22
4.2.6 Absolute normalization procedure applied to NDVI 23
4.2.7 Inter-satellite cross-calibration (if using images from different satellites) 24
4.2.8 Clouds and shadows mask 24
4.2.9 RGB color composite 24
4.3 Computing biophysical parameters 25
4.3.1 Leaf Area Index (LAI):theoretical background 26
4.3.2 Model calibration 27
4.3.3 Surface Albedo (r) or Spectrally integrated hemispherical reflectance: Theoretical background 29
4.3.4 Evapotranspiration under standard conditions (ET_p): Theoretical background and equations 30
4.3.5 direct calculation of ETp 31
4.3.6 crop coefficient approach 32
4.3.7 Irrigation Water Requirements (IWR) 33
4.4 Images classification 33
4.5 Evapotranspiration maps 33
5. Results 35
6. Validation 36
7. Web-GIS 37
8. Landscape aspects 39
8.1 Greece study area 39
8.2 italy study area 40
9. References 43
Annex 1 44
detail on images aquisition 44
Annex 2 48
Detail on Leaf Area Index measurement 48

List of Figures

Figure 1- REGION OF APULIA (ITALY) AND REGION OF EPIRUS AND WESTERN GREECE (GREECE) 9
Figure 2 - Italian study area 12
Figure 3 - greece study area 13
Figure 4 - LICOR canopy analyser for LAI measurements 14
Figure 5 - trend OF annual MEDIUM TEMPERATURE AND rainfall for the years 2013 (a) and 2014 (b). Andria Station Italy 15
Figure 6 - TREND OF ANNUAL ET0 and rainfall events for the years 2013 (a) and 2014 (b). Andria Station Italy 16
Figure 7 - TREND OF ANNUAL MEDIUM TEMPERATURE AND RAINFALL FOR THE YEARS 2013 . KOMPOTI STATION Greece 17
Figure 8 - TREND OF ANNUAL ET0 AND RAINFALL EVENTS FOR THE YEARS 2013. KOMPOTI STATION GREECE 17
Figure 9 - Method for ETp and Kc using in situ and satellite remotely data 19
Figure 10 –NDVI maps FOR LANDSAT 8 OLI. a) Italy DATE 10/08/2014. b) greece date 05/08/2014 23
Figure 11 – FAlse Color composite maps for Landsat 8 OLI – a) Italy DATE 10/08/2014. b) greece date 05/08/2014. different tones of red denote the spatial variability of crop development 25
FIGURE 12 - lai maps FOR LANDSAT 8 OLI. a) Italy DATE 10/08/2014. b) greece date 05/08/2014 26
Figure 13 - Field measurements of Leaf Area Index (LAI) 27
Figure 14 - Leaf Area Index (LAI) estimated (Y) versus LAI measured (X) 28
FIGURE 15 - albedo maps FOR LANDSAT 8 OLI. a) Italy DATE 10/08/2014. b) greece date 05/08/2014 29
Figure 16 - Scheme for analytical approach of Kc determination from E.O. data 30
Figure 17 - Example of ETp cumulated in an area 34
Figure 18 -CWR maps in the study area available in Web-GIS system. 35
Figure 19 - IRMA IRrigation MAnagement: main page 37
Figure 20 - Query data frame: table and graphs 38

List of Tables

Table 1- Images aquired IN 2013 AND 2014 for the project 15
Table 2 - Sampling characteristics of EO satellites (VHR-HR-MR range).VIS: visible; NIR: near-infrared; SWIR: short-wave infrared; TIR: thermal infrared. 20
Table 3 - SUMMARY OF false COLOR COMPOSITION RECOMMENDED BANDS AND CHANNELS FOR VARIOUS SENSORS. 25
Table 4 - Weighting coefficients for the calculation of albedo (r) by using Eq. (9) and surface reflectance derived from Landsat 8 OLI 29
Tabel 5 - Sample albedos 30
Table 6 - Maps derived from satellite images divided by area 35
Table 7 - RIEPILOGO DEI DATI STATISTICI PER LE MAPPE DI EVAPORAZIONE CUMULATE PRODOTTE PER STAGIONE IRRIGUA E PER AREA DI STUDIO 35
Table 8 –Location of landscape identified in greece study area 39
Table 9-urban landscape: target " Football field" 40
Table 10 - urban landscape: target " public park" 41
Table 11- urban landscape: target “tennis field” 42
Tabella 12 - TABLE 11- URBAN LANDSCAPE: TARGET “golf FIELD” 42
Table 13 - LANDSAT 8 OLI - PUGLIA ITALY 44
Table 14 - RAPID-EYE - PUGLIA ITALY 46
Table 15- RapidEye and related mosaic - PUGLIA ITALY 46
Tabella 16 - LANDSAT 8 OLI - greece 47
Tabella 17 - Rapid-Eye – Greece 47
Table 18 - Field measurements of Leaf Area Index (LAI) 48

List of Symbols and Acronyms

Symbol/ Acronyms	Interpretation	Unit
CLAIR	Clevers' Leaf Area Index by Reflectance model	
CWR	Crop Water Requirements	mm, m^3
d	Day	
d	Earth sun distance	a.u
DN	Digital number (quantum radiance)	-
ET_0	Reference evapotranspiration	mm/d
ET_p	Crop evapotranspiration	mm/d
$ESUNi$	Extraterrestrial solar irradiance for band i	Wm^2 /µm
GPS	Global Position System	m
GSD	Ground Sample Distance	m
h_c	Crop height	m (0.12 for reference crop)
h_c^*	Crop height	m (constant value of 0.4 m in this study)
IWR	Crop Water Requirements	mm, m^3
K_c	Crop coefficient	-
L_i^e	Spectral radiance in band *i*	Wm^2 /sr/µm
LAI	Leaf area index	
LAI*		m^2/ m^2 (estimated from satellite)
NDVI	Normalized difference vegetation index	-
OLI	Operational Land Imager	m^2/m^2 (2.88 for reference crop)
WDVI	Weighted Difference Vegetation Index	-
WDVI∞	Weighted Difference Vegetation Index for fully covering canopies	-
P	Actual precipitation	mm/d
P_n	Net precipitation	mm/d
r	Surface albedo	- (0.23 for reference crop)
*r**	Surface albedo	- (estimated from satellite)
R^2	Coefficient of determination	-
RH	Air humidity	%
RMSE	ROOT-MEAN-SQUARE ERROR	-
SIMODIS	SImulation and Management of On-Demand Irrigation System	
ρi	Canopy reflectance in the near infrared channel	-
ρr	Canopy reflectance in the near infrared channel	-
ρsi	Soil reflectance in the near infrared channel	-
ρsr	Soil reflectance in the near infrared channel	-
S	Solar radiation	W/m^2
SAVI	Soil Adjusted Vegetation Index	-
T_a	Air temperature	°C
U	Wind speed	m/s
VI	Vegetation Index	-
a	Crop saturation per unit foliage area	cm/d
α*	Extinction coefficient for LAI estimation	-
θs	Sun zenith angle	rad

IRMA project aims at developing innovative and new service capacities within the Earth monitoring program GMES[1] for the broad agricultural user community of both rainy and irrigated agriculture and sustainable food production, in accordance with the vision of bridging and integrating sustainable development and economic competitiveness.

The objective of the activities 6.3.3 is to estimate crop evapotranspiration (ETp) by using Landsat 8 and RapidEye satellite data in combination with meteorological data and field measurements and by adopting the FAO-56 (Allen, 1998) approach in two study area, one in Italy (Apulia Region) and one in Greece (Region of Epirus). The accurate estimation of evapotranspiration is needed to improve irrigation efficiency and to achieve water savings, with special concern in arid and semi-arid climatic conditions. Among other techniques, the analysis of remote sensing data in relation to crop water requirements and irrigation scheduling has become a topic of increasing research attention in recent years, either by using satellite-based spectral indices either by investigating the relationships between energy fluxes, spectral reflectance and crop coefficients.

FIGURE 1- REGION OF APULIA (ITALY) AND REGION OF EPIRUS AND WESTERN GREECE (GREECE)

[1] Global Monitoring Environment and Security (GMES), now Copernicus is the European Programme for the establishment of a European capacity for Earth Observation

1. REMOTE SENSING FOR DETERMINING CROP WATER REQUIREMENTS FROM SATELLITE OPTICAL DATA: METHODOLOGICAL BACKGROUND

The commonly accepted equation for estimating crop evapotranspiration (ETp or Crop Water Requirements - CWR), according to the schematization of FAO-paper 56 (Allen et al., 1998), is a function of climate data such as temperature (T), humidity (RH), solar radiation (S) and wind speed (U) and crop parameters, such as the surface albedo (r), the leaf area index (LAI) and the crop height (hc), the so called "*one-step approach*":

$$ETp = f\{r, LAI, hc|Ta, RH, S, U\} \quad (1)$$

Satellite remotely sensed – and more in general Earth Observation (E.O.) - data provide a real-time assessment of the magnitude and variation of crop condition parameters, and this study investigates the use of remote sensing on estimations of r, LAI and hc as an input to ETp-FAO model.

Several studies shows that crop parameters involved in the evapotranspiration process can be estimated trough spectral measurement in the visible (VIS) and near infrared (NIR) spectral regions from medium/high resolution satellite images, due the strong relationship between the spectral response in those region of the electromagnetic spectrum of cropped surfaces and the corresponding parameters values (D'Urso, Calera, 2006).

This approach would eliminate the calculation of the *Kc* in the procedure known as *single Kc approach* (Allen et al., 1998), ETp is calculated, starting from reference evapotranspiration ETo assuming an ideal crop with standard parameters (hc=0.12 m, r =0.23, LAI=2.88 m^2/m^2) and a crop coefficent *Kc* extract from table;

$$ETp = ETo\ Kc \quad (2)$$

with:

ETp crop evapotranspiration [mm/d]
Kc crop coefficient [dimensionless]
ETo reference evapotranspiration [mm/d]

Nevertheless, due to wide use of *Kc* in irrigation practice, it is possible to derive a physically-based *Kc* expressed as an explicit function of the canopy properties, LAI, r and hc, and of the meteorological data (D'Urso and Menenti, 1995).

$$Kc=ETp/Eto \quad (3)$$

The crop coefficient, *Kc* incorporates, and synthesizes all the effects on the evapotranspiration related to morpho-physiological characteristics of the different crops, phenological stage, degree of soil cover, soil and climate conditions, which make them different from the reference crop.

Kc values are extremely variable, even within the same type of crop, depending on many factors, i.e. date and seeding density, intake of nutrients, nature of the soil, agronomic

practices. In order to assess the spatial/temporal variability of the *Kc*, in the IRMA project a methodology based on calculation of *Kc* from Remote Sensing (RS) techniques is proposed (D'Urso, Calera, 2006).

This research report describes the materials, procedures and the results of experimental evaluation of evapotranspiration and *Kc* of agricultural areas and urban landscape (as golf club, parks, football fields, etc..) in the two study areas during the irrigation period in 2013 and 2014.

This report has been structured in the following section:

1. Study area description;
2. Resources committed;
3. Methodology, quick guide to EO basic processing and core product generation. This part provides an overview of the entire process ranging from the selection of images to the calculation of advanced biophysical parameters. The basic procedure for each product is summarized here, including in most cases the models or equations.

2. STUDY AREA

The operational campaign was carried out in the two pilot area (Apulia and Epirus), using satellite images and ancillary information such as available output from agro-meteorological stations, vector maps of plots, field work & surveys to validate the process.

The Italian study area is located in Apulia Region, in the south eastern part of Italy, with a large cultivated areas. Apulia is mainly dominated by agriculture, with more than 70% of the total area occupied by cropped land, and represent about 10% of Italian Utilized Agricultural Area (UAA). The water resources derived from surface water bodies are limited, causing a major constraint to the social and economic development of the region. The regional topography is mainly flat or slightly sloping, with the exception of the Gargano area (North-West of the region). The climate variables, and rainfall in particular, exhibit a marked inter-annual variability which makes water availability a permanent threat to the economic development and ecosystem conservation of the region. Due to its geo-climatic boundary condition the region has an overall groundwater exploitation which expose the water supply system to severe water scarcity events. The study area is located within Ofanto river basin, an important agricultural district and irrigation system of the region. The area covers a surface of more 3,500 km^2 between the town of Foggia in the north-west and the town of Ruvo di Puglia in the south-east. Agriculture is characterized by fruit trees, olive grove, vineyards of wine and grapes, vegetables and orchards. The local irrigation system, is managed by two Consortium: the "Capitanata" and the "Terre d'Apulia" (irrigated districts are shown in Figure 2).

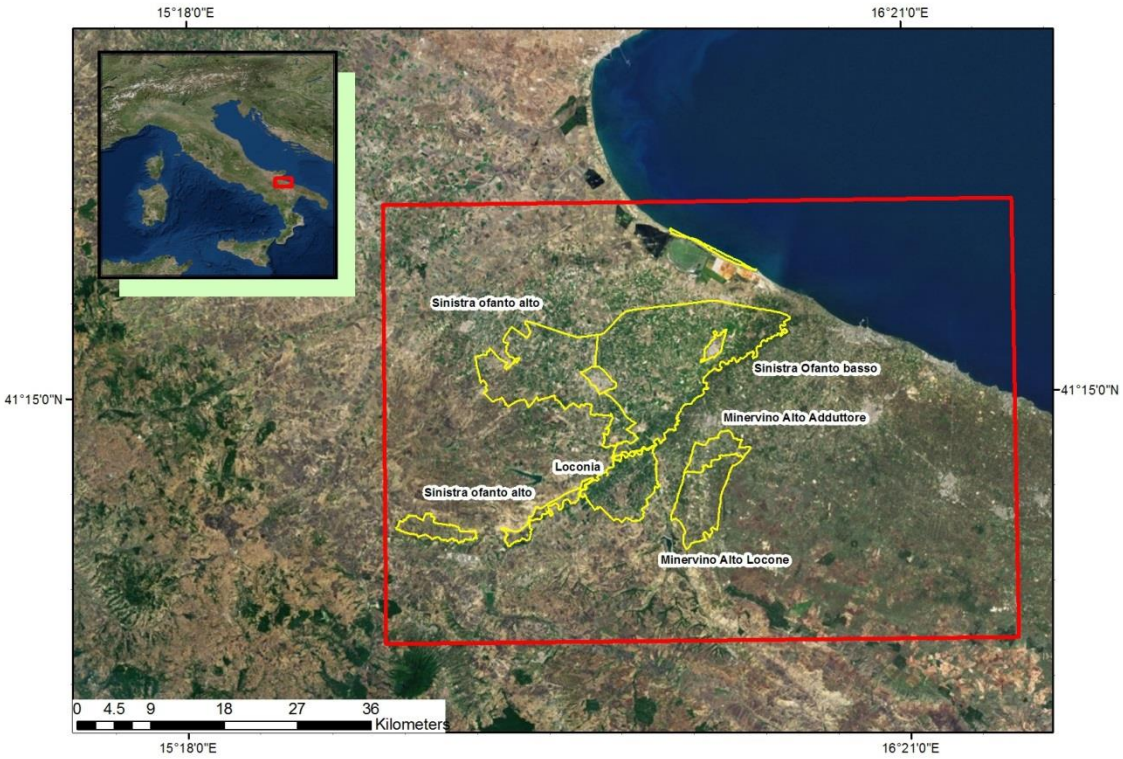

FIGURE 2 - ITALIAN STUDY AREA

The Greece study area (Figure 3) is located in the Region of Epirus, at the North-West part of Greece, it has a total area of 9.203 km^2 (agricultural land corresponds to the 14% of it). The

plain of Arta (45.329 ha, the biggest of the region) is located at the south edge of Epirus, it is part of the Aracthos and Louros hydrological basins and intersects with Amvrakikos Wetlands National Park. The main crops of the region are fruit trees, olive groves, rice fields and complex cultivation patterns (Corine land cover, 2000) that comprise from vegetables, cotton and other annual cultivations. The climate of Arta's plain is of Mediterranean type, with hot summers and rainy moderate winters.

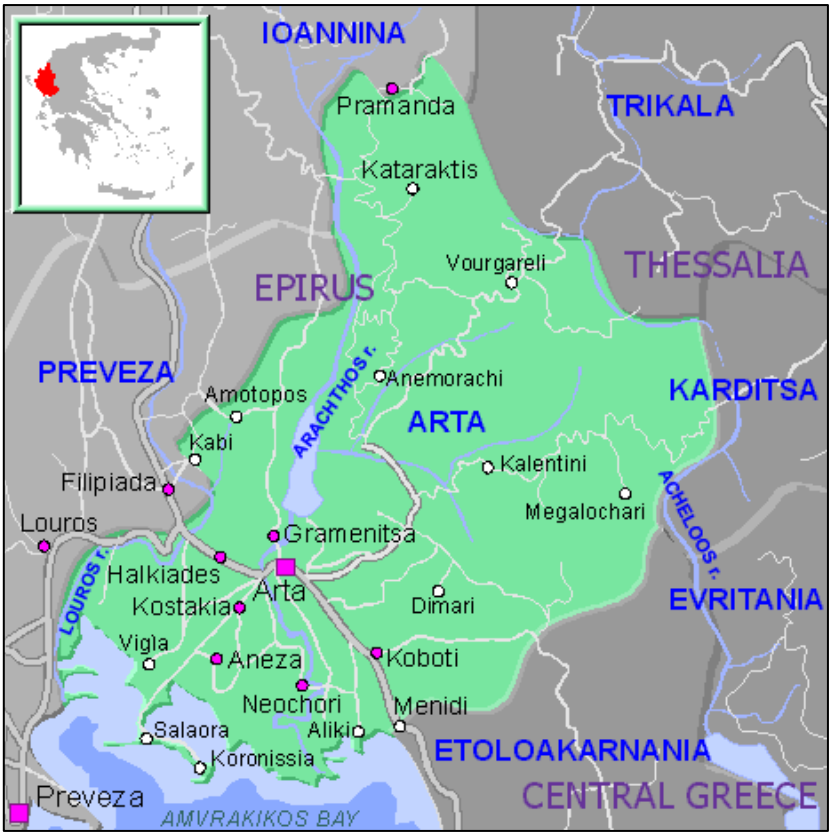

FIGURE 3 - GREECE STUDY AREA

3. RESOURCES

3.1 LICOR LAI-2000 PLANT CANOPY ANALYZER

Leaf Area Index is commonly used for monitoring crop growth. Instead of the traditional, direct and labor-consuming method of physically measuring the plant with a ruler (direct method), an optical instrument, LICOR LAI-2000 Plant Canopy Analyzer (Figure 4), is used (indirect method). The LAI-2000 (Li-Cor inc., Lincoln, USA) uses a fish-eye lens with an hemispheric field of view (±148º). The detector is composed of five concentric rings (sensitive to radiation below 490 nm). Each ring responds over a different range of zenith angles. Light attenuation through the canopy is measured and light transmittance is calculated as the ratio of below: above canopy readings for each of the 5 angles. This ratio is used to calculate several variables, including leaf area index, gap fraction, and mean tilt angle (a number representing the foliage orientation). Fractional vegetation cover can be also computed from these data.

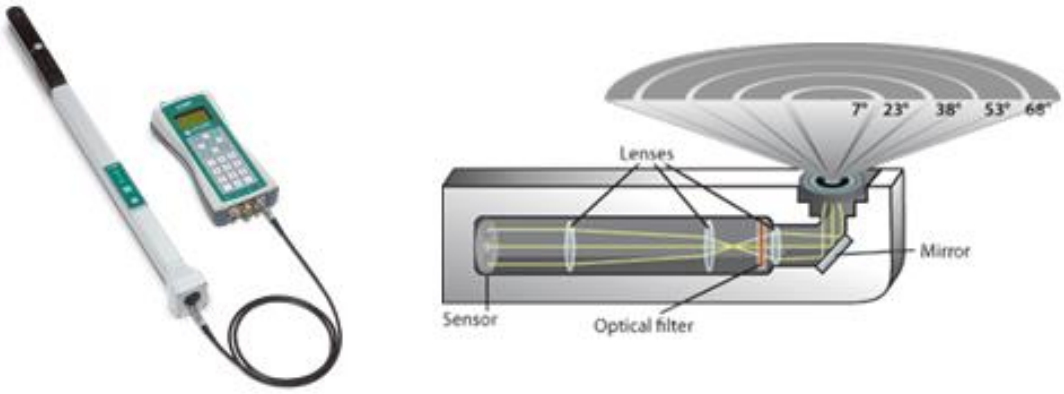

FIGURE 4 - LICOR CANOPY ANALYSER FOR LAI MEASUREMENTS

3.2 SATELLITE IMAGES

Earth Observation data used in this study are represented by a set of images collected by the sensor OLI (Operational Land Imager), mounted on-board the Landsat 8 Mission (formerly the Landsat Data Continuity Mission, LDCM); each individual OLI image covers the entire study area, with a medium geometric resolution (30 m).

In addition, several RapidEye high resolution images (6.5 m, resampled at 5 m) were acquired to improve temporal resolution of Landsat data, according to the concept of virtual constellation (consisting on using different sensors), allowing for monitoring the vegetation development throughout the growing season.

Because the Italian area of interest concerns two frame Landsat 8 (path 188, row 31 and path 188, row 32), the elaborated data refer a total of 42 acquisitions. For Apulia study area, the high resolution images of RapidEye (Table 1) were acquired from 12th June to 14th July 2013 and

from 12th June 2014 to 29th September 2014 for a total of 11 dates. For Greece area, 2 high resolution satellite images were acquired in 2014, respectively in June and July.

In Table 2 there is a summary of the images acquired for the project.

TABLE 1- IMAGES AQUIRED IN 2013 AND 2014 FOR THE PROJECT

Data	Study area	Satellite	N. images	N. date	Period
Earth observation	Apulia (Italy)	Landsat-8 OLI	42	21	19/5/2013 – 27/09/2014
		Rapideye	11	11	12/06/2013 - 29/09/2014
	Artha (Grecee)	Landsat-8 OLI	21	21	12/04/2013 - 22/09/2014
		Rapideye	2	2	12/06/2014 and 22/07/2014
Total			76	55	

Detailed description of images acquisition are reported in Annex 1

3.3 METEREOLOGICAL DATA

In Italy, meteorological data were acquired from five station managed by "Assocodipuglia", the agrometeorological service of Apulia Region. Rainfall and temperature in 2013 and 2014 were slightly different but in accordance with climatological averages for the study area (Figure 5). The year 2013 has been characterized by rainy winter and spring and dry summer, with anomalously high precipitation in august and in autumn, while 2014 experienced a rainy spring, where long term average precipitation from April to June was 210 mm, about 35% of the annual amount. This situation affected the crop water requirements during the growing season. Annual rainfall and mean temperature were 629.2 mm and 16.2°C for 2013, and 607.4 mm and 16.7°C for 2014, respectively. Total rainfall from 1 June to 30 September was 114.4 mm (18% of the annual amount) in 2013 and 103 mm (27% of the annual amount) in 2014, respectively.

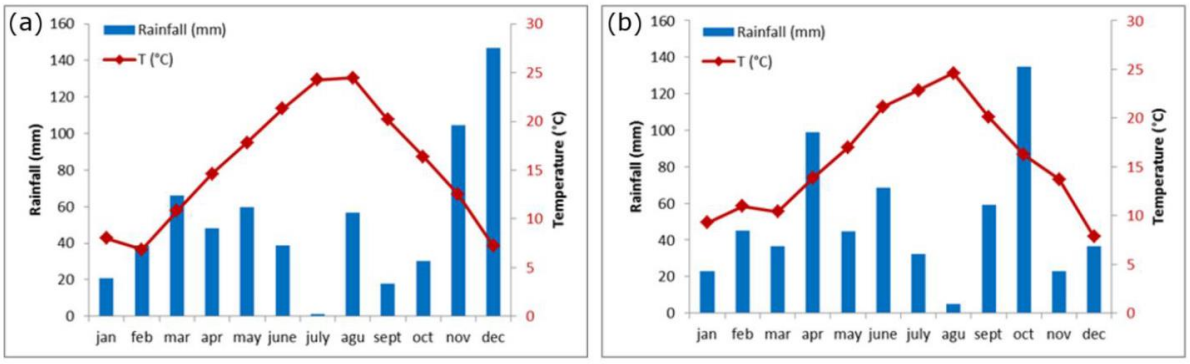

FIGURE 5 - TREND OF ANNUAL MEDIUM TEMPERATURE AND RAINFALL FOR THE YEARS 2013 (A) AND 2014 (B). ANDRIA STATION ITALY

Seasonal variations of ETo are shown in Figure 6 for 2013 and 2014, respectively. The total amounts of ET0 in the growing season (1 June to 30 September) were very similar in both investigation years, 511 mm in 2013 and 501.6 mm in 2014. The average daily ETo was 4.2

mm/d and 4.1 mm/d in the first and second year respectively. In the growing season 2013 the lowest daily ETo was mm/d (30 September 30) and the highest was 6.7 mm/d (24 June). In the growing season 2014, ET0 values ranged from 1.7 mm/d (1 September) to 6.7 mm/d (29 June).

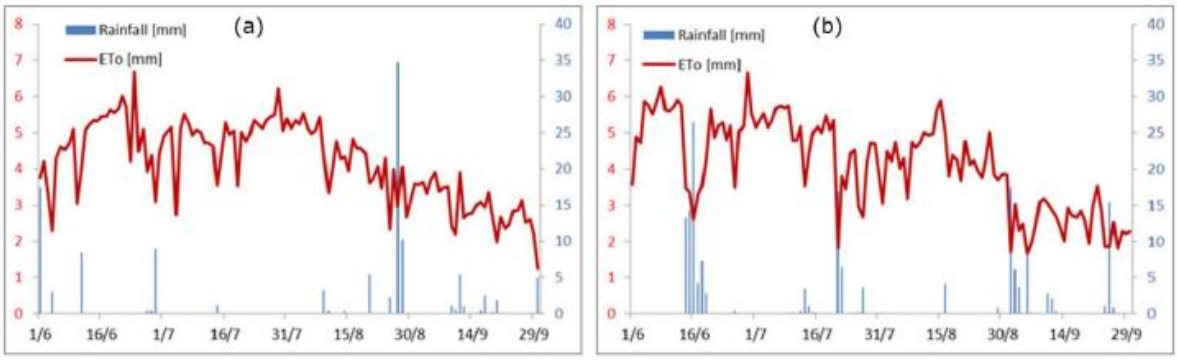

FIGURE 6 - TREND OF ANNUAL ET0 AND RAINFALL EVENTS FOR THE YEARS 2013 (A) AND 2014 (B). ANDRIA STATION ITALY

Metereological data collected in Apulia Region are the following:

1. ET T Evapotranspiration, daily data [mm]
2. PA M Atmospheric pressure , average, daily data [hPa]
3. PC T Rainfall, total, daily data [mm]
4. RG T Global radiation, total, hourly data [kJ/m]
5. RG T Global radiation, total, daily data [kJ/mq]
6. TC H Temperature 2 M MAX, daily data [°C]
7. TC L Temperature 2 M MIN, daily data [°C]
8. TC M Temperature 2 M average, daily data [°C]
9. UC H Relative humidity 2 M MAX, daily data [%]
10. UC L Relative humidity 2 M MIN, daily data [%]
11. UC M Relative humidity 2 M average, daily data [%]
12. VA M Wind speed 10 M average, daily data [m/s]
13. VB M Wind speed 2 M average, daily data [m/s]

In Greece, meteorological data were acquired from 3 meteorological station:

- from 1/5/13 to 30/11/13: Vlacherna and Kompoti
- from 1/5/13 to 2/8/13: Arta near Technological Educational Institute (TEI).

Rainfall and temperature in 2013 (Figure 7) shows a typical Mediterranean trends with rainy autumn and winter and dry summer. Annual rainfall and mean temperature were 995.2 mm and 18.5°C, respectively. Total rainfall from 1 June to 30 September was 88.6 mm (0.08% of the annual amount).

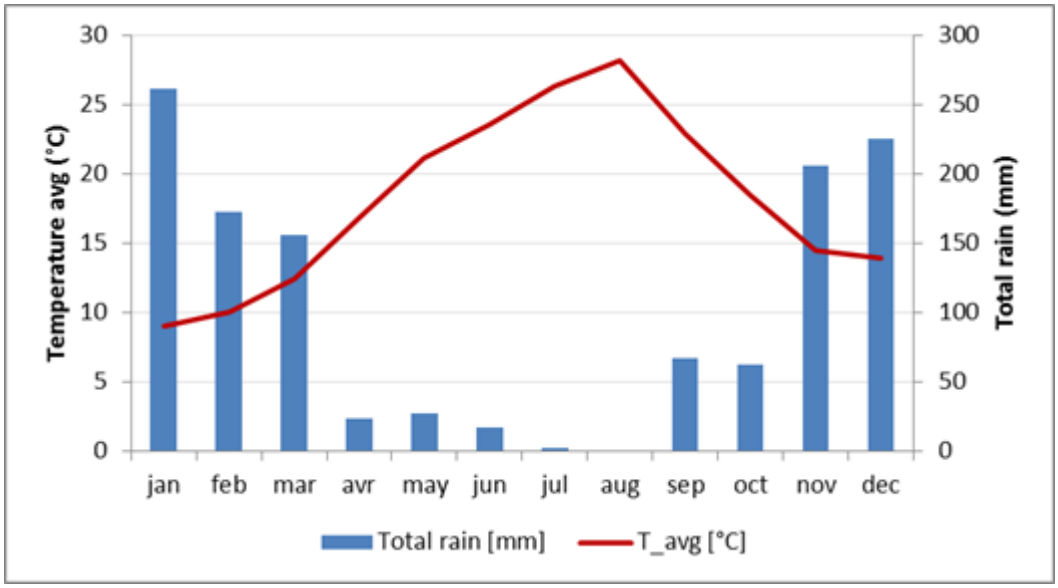

FIGURE 7 - TREND OF ANNUAL MEDIUM TEMPERATURE AND RAINFALL FOR THE YEARS 2013 . KOMPOTI STATION GREECE

Seasonal variations of ETo are shown in Figure 6 for 2013. The total amounts of ETo in the growing season (1 June to 30 September), 523 mm (68% of the annual ETo). The average daily ETo was 4.3 mm/d. In the growing season, the lowest daily ETo was 1.9 mm/d (30 September) and the highest was 5.7 mm/d (18 June).

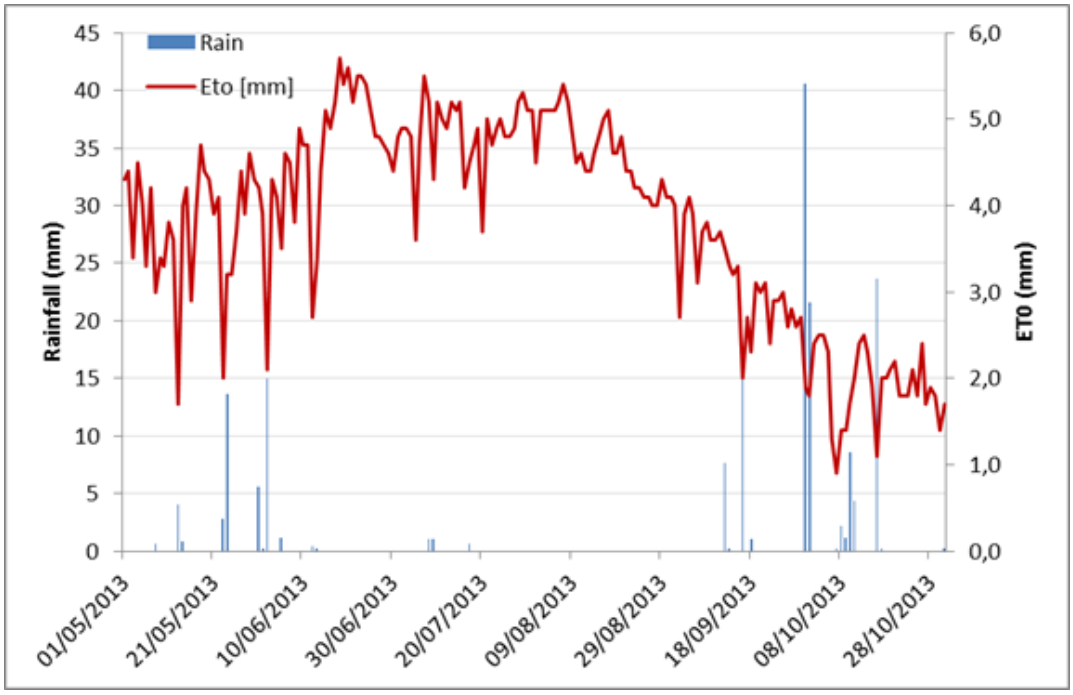

FIGURE 8 - TREND OF ANNUAL ET0 AND RAINFALL EVENTS FOR THE YEARS 2013. KOMPOTI STATION GREECE

Metereological data collected in Greece are the following:

1. PC T Rainfall, total, daily data [mm]
2. RG T Global radiation, total, hourly data [kJ/m]
3. TC H Temperature 2 M MAX, daily data [°C]
4. TC L Temperature 2 M MIN, daily data [°C]
5. TC M Temperature 2 M average, daily data [°C]
6. UC H Relative humidity 2 M MAX, daily data [%]
7. UC L Relative humidity 2 M MIN, daily data [%]
8. UC M Relative humidity 2 M average, daily data [%]
9. VB M Wind speed 2 M average, daily data [m/s]

3.4 ANCILLARY DATA

Other ancillary and administrative data were used to support elaborations, for instance Consortium information, land use/cover map of the 2 study area: "*Carta dell'utilizzazione Agricola del suolo*" (CUAS) for Italy and Corine Land Cover for Greece, etc.

4. METHODOLOGY

The methodology followed in this study was structured in four steps:

1. Selection and purchase of images;
2. Preprocessing of images, that was implemented in software such as Intergraph ERDAS Imagine ®;
3. images Classification
4. Calculation of biophysical parameters;

The flow diagram gives an overview of the sequence of sub-steps followed. Each sub-step is detailed in the paragraphs below.

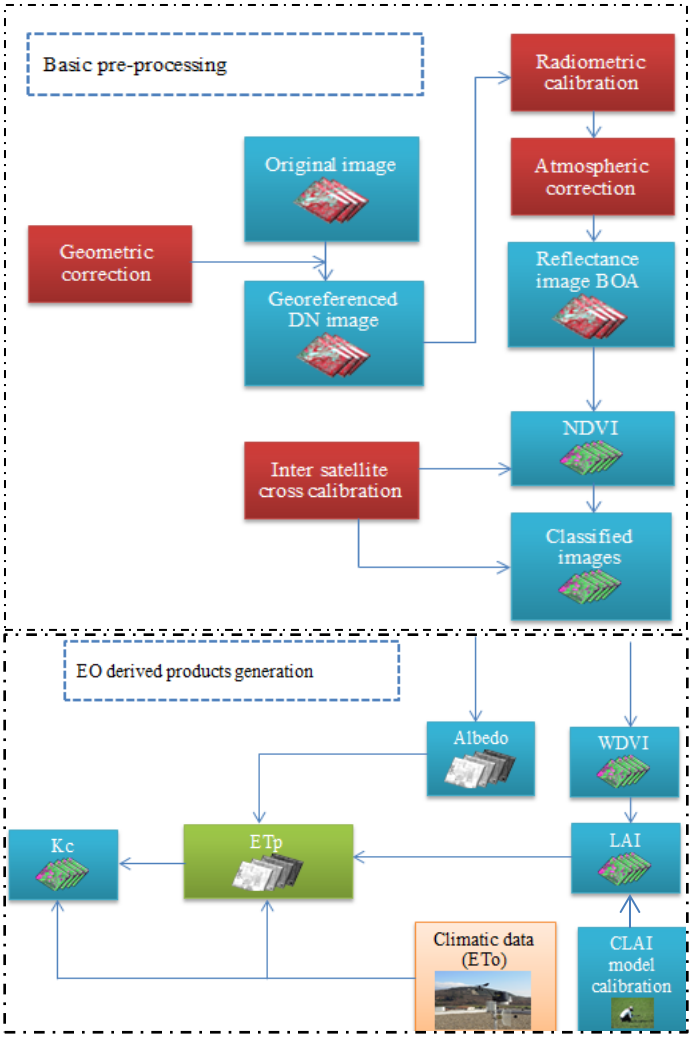

FIGURE 9 - METHOD FOR ETP AND KC USING IN SITU AND SATELLITE REMOTELY DATA

4.1 SELECTION AND PURCHASE OF IMAGE

4.1.1 BASICS

The virtual satellite constellation has been defined as the ensemble of all EO satellites currently in orbit that satisfy the temporal, spectral, radiometric and spatial resolution requirement for a given application. **Errore. L'origine riferimento non è stata trovata.** 2 gives an overview of satellites with Very High (VHR) and High (HR) resolution that are used in the project and are adequate for agricultural application. For intercalibration of measurement from different sensors at different observation scales in different platforms the methodology developed by Martínez-Beltrán et al. (2009), is applied.

TABLE 2 - SAMPLING CHARACTERISTICS OF EO SATELLITES (VHR-HR-MR RANGE).VIS: VISIBLE; NIR: NEAR-INFRARED; SWIR: SHORT-WAVE INFRARED; TIR: THERMAL INFRARED.

Satellite	Repeat cycle	Image size	Bands (number)	GSD* (m)
Landsat 8 OLI TIRS	16 days	185 km x 185 km	VIS (4)	30
			NIR (1)	30
			Cirrus (1)	30
			SWIR (2)	30
			TIR (2)	100
Rapid-Eye constellation	Up to daily	25 km x 25 km	VIS (4)	6.5
			NIR (1)	

Note: *Ground sample distance

At the beginning of the project it was made a calendar of overpasses of all satellites for the study areas (including a map, .shape or .jpg, of the areas covered by all different scenes) e.g., Landsat calendar: http://landsat.usgs.gov/tools_L8_acquisition_calendar.php. Then the images to be purchased or ordered (some satellite acquisitions need to be programmed beforehand), were selected and ordered from local distributors. The selection of satellite images was done following 3 main criteria:

- Resolution: as a rule of thumb, a HR satellite/sensor (of around 30m pixel size) can "see" parcels of 1 ha. For smaller-size fields, it's better to use VHR images.
- Cost: for most satellites, there are regional or national distributors where images can (or in some cases must) be purchased. Prices can vary considerably from region to region and for any given satellite, images can be expensive in one region and low-cost in another region.
- Operational delivery: the image distributor should be able to deliver images within 24-48 hours after overpass.

4.2 PRE-PROCESSING OF IMAGES

4.2.1 GEOREFERENCING

The geographical reference system used in the project IRMA is Datum: WGS 84; Projection: UTM. The transformation coefficient for the coordinates are derived by using ground control points methodology. Ground control points methodology requires the use of a reference-master image, these images may be ortho-photographs, rectified satellite images, etc. A complete collection of orthorectified satellite images may be found in ftp://ftp.glcf.umiacs.umd.edu/glcf/.

The resampling method used is Nearest Neighbor technique.

4.2.2 IMAGE RADIOMETRIC CORRECTION

Since multi-temporal images are often acquired by different sensors under variable atmospheric conditions, solar illumination and view angles, radiometric normalization is required to remove radiometric distortions and make the images comparable.

Reflectance at satellite (apparent reflectance) is the main magnitude derived from satellite images.

$$\rho_i = \frac{\pi * L_i^e * d^2}{k * ESUN_i * \cos\theta_s} \quad (4)$$

where k is the correction factor due to the eccentricity of the Earth orbit and d is the Earth-Sun distance, θs sun zenith angle, L_i^e is spectral radiance in band i (in W/m²/sr/μm). *ESUNi* is the extraterrestrial solar irradiance for band i (in W/m²/μm). Its calculation requires an intermediate process to convert digital numbers, DN, registered by the sensor in at sensor spectral radiances, L_i^e. Conversion of DN to L_i^e depends on the sensor analyzed. For Rapid-Eye, OLI/TIRS the following equation is computed:

$$L_i^e = a_{1,i} * DN_i + a_{0,i} \quad (5)$$

where $a_{0,i}$ and $a_{1,il}$ are the sensor calibration coefficients for the band i (Chander et al. 2009).

4.2.3 ATMOSPHERIC CORRECTION

The conversion of a satellite signal to a land signal requires the use of any atmospheric correction methodology. This step is highly recommended to ensure satellites comparability, time series stability and the compatibility between the different approximations to derive biophysical parameters.

Current atmospheric correction methodologies can be divided into absolute. Absolute correction methods try to eliminate or compensate atmospheric distortion in radiometric signal using atmosphere properties at satellite acquisition time and radiance inversion models

(Guanter et al. 2007). Relative atmospheric correction methods normalize the signal obtained in a satellite time series to the signal of one single of a cluster of images considered as reference, this normalization is usually performed using the signal measured over target surfaces considered pseudo-invariant. Each single band is normalized respect to the reference (Schroeder et al. 2006) or the combination of multiple bands into vegetation indices are corrected respect to this reference (Chen et al. 2005).

In area where many invariant features are present, the relative correction can be applied after absolute corrections to improve the smoothness of the time series, correcting errors of the first correction due to uncertainties in atmospheric parameters.

4.2.4 MOSAICKING

In Apulia Region the area of interest concerns two frame Landsat 8 (path 188, row 31 and path 188, row 32), for this reason a mosaic of acquired images was done: 42 acquisitions were produced 21 mosaic dataset.

The acquisition of RapidEye images were very close in terms of time, so we proceeded to a mosaicking in order to minimize the cloud cover. To reduce the sensor radiometric discontinuities, in the vicinity of the areas of overlap, a normalization procedure of the linear type and a subsequent balancing for the removal of color distortions, ensuring the homogeneity of the photometric final mosaic, has been applied. When it has not been possible to apply this procedure to the areas of overlap, for example to the presence of clouds, the homogenization of the mosaic using the target time invariant (pseudo invariant features, PIFs), according to the procedure of inter-calibration, was done.

4.2.5 VEGETATION INDICES

The most common strategies to extract quantitative information on land surface biophysical parameters from remotely sensed data are based on vegetation indices (VI) (Gilabert et al., 2010). Vegetation indices are usually dimensionless measures derived from radiometric data that are primarily used to indicate the amount of green vegetation present in a view (Hamlyn, 2010). These indices, which combine reflectance values from different wavebands in the solar region, are designed to be sensitive to vegetation and insensitive to other factors acting as noise (such as atmosphere and canopy background). Most VIs exploit the fact that green vegetation strongly absorbs solar radiation in the visible region (due to the presence of chlorophyll and other pigments) and strongly reflects solar radiation in the Near Infrared (NIR) waves. They capitalize then the strong reflectance gradient exhibited by live green vegetation around 0.7 μm. Although a large number of spectral Vis have been proposed in the literature, the Normalized Difference Vegetation Index (NDVI), introduced by Rouse et al. (1974), is the most popular and the most widely used in remote sensing applications related to global studies, crop management, land cover studies and climate studies (Gilabert et al., 2010).

$$NDVI = \frac{\rho_{NIR} - \rho_R}{\rho_{NIR} + \rho_R} \quad (6)$$

with ρ_{NIR} and ρ_R reflectance in NIR and RED respectively. NDVI is used to distinguish between vegetated surfaces (NDVI>0.3), bare soils (0.01<NDVI<0.2 and water (NDVI<0.0).

FIGURE 10 –NDVI MAPS FOR LANDSAT 8 OLI. A) ITALY DATE 10/08/2014. B) GREECE DATE 05/08/2014

For derivating vegetation products, a different VI is used in RapidEye, which consider a correction for the influence of the soil surface underlying the vegetation cover. The Weighted Difference Vegetation Index (WDVI) was firstly introduced by Clevers (1989) and defined as follows:

$$WDVI = \rho_i - \rho_r \frac{\rho_{si}}{\rho_{sr}} \quad (7)$$

where ρ_i and ρ_r indicate the reflectance of the observed canopy in red and infrared bands, respectively, while ρ_{si} and ρ_{sr} are the corresponding values for bare soil conditions.

4.2.6 ABSOLUTE NORMALIZATION PROCEDURE APPLIED TO NDVI

Calibration procedure is based on direct relationships between sensors response and ground spectral response for reference surfaces. Assuming bare soil and dense green cover as NDVI-near invariant, the ground-based NDVI values for bare soil and dense green cover could be used to calibrate NDVI values from the sensor by means of a linear relationship. To apply this procedure, patches of bare soil and dense green cover need to be present and identified into the image. Typical NDVI value for agricultural bare soil is around 0,14 and NDVI value for dense green vegetation cover is around 0,91 (Landsat bandwidths). Absolute normalization procedure applied to the NDVI could provide a coherent time series of images from multiple sensors, and could provide an operational complementary procedure when the assumption about the presence on images of bare soil and dense green vegetation is satifisted.

4.2.7 INTER-SATELLITE CROSS-CALIBRATION (IF USING IMAGES FROM DIFFERENT SATELLITES)

The joint use of multi-resolution sensors offers many opportunities for vegetation studies; however, it requires inter satellite cross-calibration. The convenience of inter-satellite cross-calibration is based in the ability to combine spatial information of different sensors. Steven et al. (2003) published a complete collection of cross-calibration relations based on satellite sensors spectral response simulations. Martínez-Beltrán et al. (2009) show the possibility of comparing the information from different sensors using adequate spatial scale of satellite-derived vegetation indices. This study concludes linear relations between Normalize Difference Vegetation Indices (NDVI) derived from Landsat-7 ETM+ and various sensors. Similar relations may be derived for different sensors if near-synchronous pairs of images are available.

4.2.8 CLOUDS AND SHADOWS MASK

The presence of clouds and shadows over the study area at satellite acquisition time disturbs the signal acquired by the sensor. The signal below the cloud-shadow is unrecoverable, and the proposed solution is to substitute the disturbed pixels value by an unrealistic value, i.e. 9999, and to avoid the unrealistic values in the calculation of biophysical parameters.

Some semiautomatic models based on clouds and shadows reflectance and temperature have been developed (Hagolle et al. 2010; Lyapustin et al. 2008), but the accuracy and applicability of each model to a specific sensor and conditions must be evaluated. An alternative is the generation of a cloud mask based in the visual interpretation of the image.

4.2.9 RGB COLOR COMPOSITE

Multi spectral images are usually displayed in the form of colour composites. It is only feasible to view the information from three channels at once using conventional three-colour display systems (Hamlyn, 2010). Therefore, 3 of the bands are selected and each displayed on one of the colours of the monitor. The most obvious combination is to display the red, green and blue channel in the R, G and b screen colour to give a natural colour composite.

A standard false composite where R= NIR, G=Red and B=Green is a helpful product in the application of remote sensing techniques. No standard procedures are available but some considerations may be having into account; studied elements must be easily identified and the composite must be stable and comparable in the time.

Color composite based on the combination of Shortwave infrared band, SWIR, in the red channel, Near infrared band, NIR, in the green channel and Red band in the blue channel allows to identify natural surfaces, soil, vegetation, etc. Since color composite is a visual tool some filters or data stretching techniques may be applied in order to enhance its desirable characteristics. Its filters must be applied by the user and should be standard and reproducible for the images in a complete temporal series (Figure 11).

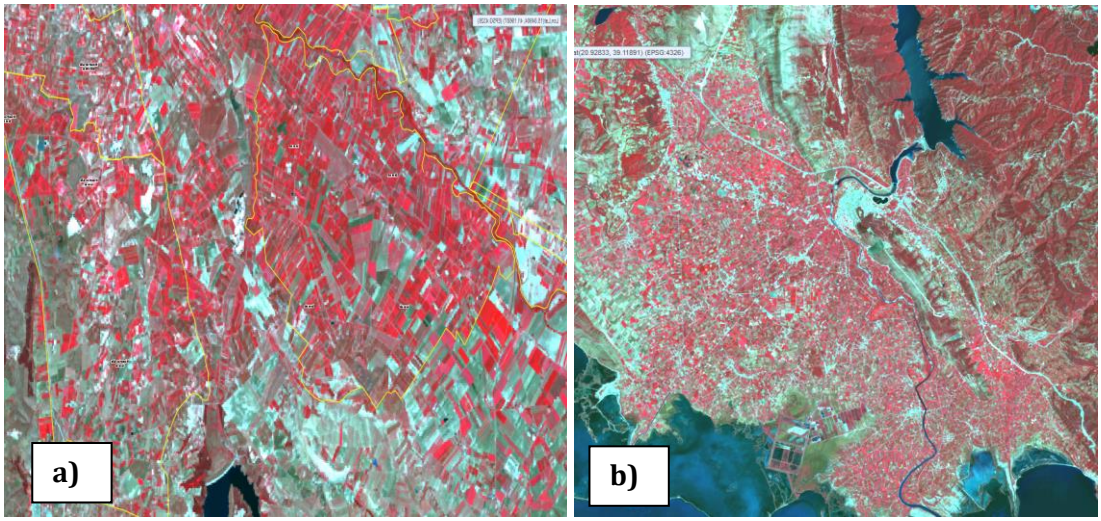

FIGURE 11 – FALSE COLOR COMPOSITE MAPS FOR LANDSAT 8 OLI – A) ITALY DATE 10/08/2014. B) GREECE DATE 05/08/2014. DIFFERENT TONES OF RED DENOTE THE SPATIAL VARIABILITY OF CROP DEVELOPMENT

The IRMA method by default to build the false color image is described on **Errore. L'origine riferimento non è stata trovata.**.

TABLE 3 - SUMMARY OF FALSE COLOR COMPOSITION RECOMMENDED BANDS AND CHANNELS FOR VARIOUS SENSORS.

Satellite	Band in Red channel	Band in Green channel	Band in Blue channel
Landsat 8 OLI	Band 5 (NIR)	Band 4 (Red)	Band 3 (Green)
Rapid-Eye constellation	Band 5 (NIR)	Band 3 (Red)	Band 2 (Green)

4.3 COMPUTING BIOPHYSICAL PARAMETERS

This section presents the methodological basis that were used in the course of the IRMA project to compute E.O. products. The parameters described are:

- Leaf Area Index (LAI);
- Albedo (r);
- Crop Coefficient (Kc);
- Evapotranspiration under standard conditions (ETp) or Crop water Requirement (CWR);
- Irrigation Water Requirements: IWR.

4.3.1 LEAF AREA INDEX (LAI):THEORETICAL BACKGROUND

Quantification of the canopy leaf area index (LAI) and its spatial distribution provides (Figure 12) an avenue to improve the interpretation of remotely sensed data over vegetated areas. LAI is defined as the total one-sided area of photosynthetic tissue per unit of ground area (Breda, 2003; Watson, 1947). Due to the role of green leaves in a wide range of biological and physical processes, LAI represents a key parameter, characterizing the structure and functioning of vegetation cover (Scurlock et al., 2001). The LAI is sensitive to changes in canopy structure and biophysical rates caused by weather extremes (such as drought, frost and storms) or management practices, and it may modify the productivity of the crops (Breda, 2003).

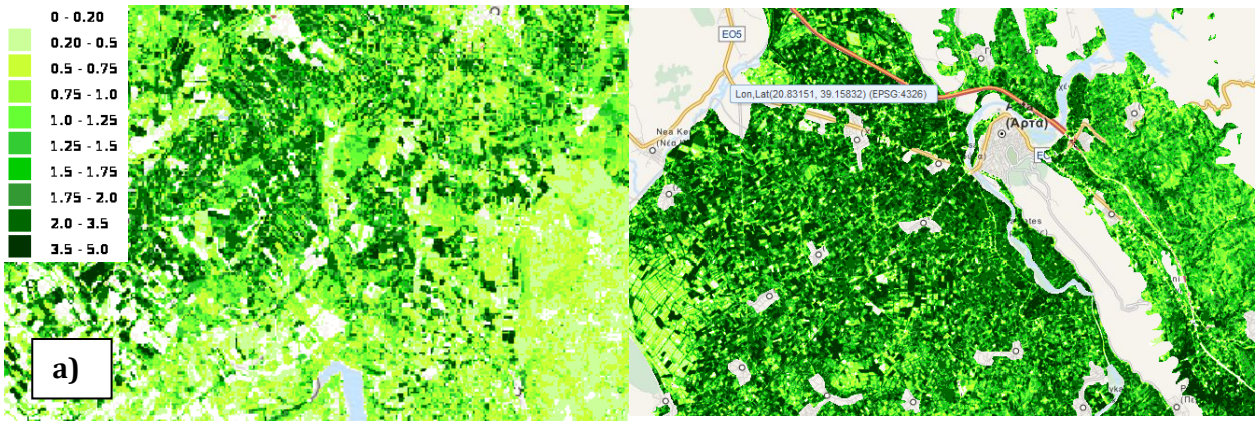

FIGURE 12 - LAI MAPS FOR LANDSAT 8 OLI. A) ITALY DATE 10/08/2014. B) GREECE DATE 05/08/2014

Three different methods are proposed for estimation of LAI from E.O. data in an operational context:

I. Traditional, simple and feasible empirical approaches, based on the relationship between LAI and vegetation indexes such as NDVI;
II. A relationship with other vegetation indices such as the CLAIR model (Clevers, 1989);
III. Analytical approach, based on the inversion of radiative transfer models (e.g. Weiss et al., 2000).

According with the different methods, the ancillary data needed for the calculation of LAI index are the following:

- Empirical/ semi-empirical methods (i, ii): LAI ground measurements for calibration purposes;
- Physical model inversion (iii):
  - ✓ Illumination and view geometry during sensor overpass;
  - ✓ soil spectrum, when available (alternatively standard spectra can be used);
  - ✓ a-priori information such as crop type and growth stage are of advantage.

In IRMA project, it was applied the simplified model CLAIR (Clevers, 1989) that is based on the Weighted Difference Vegetation Index (WDVI). Hereby, the LAI is obtained from a logarithmic relationship, by calibrating the equation (5) with ground measurements to assess the α^* value.

$$LAI = -\frac{1}{\alpha^*}\ln\left(1-\frac{WDVI}{WDVI_\infty}\right) \quad (8)$$

where α* is an extinction coefficient - empirical shape parameter, mainly depending on canopy architecture, (computed from field measurement considerate as 0.39 in this study), WDVI∞ is the asymptotical value of WDVI for LAI→∞, and is calculated at each acquisition at the target "vegetation cover (not woody) very dense and uniform" or maximum vegetation (agricultural) cover (usually between 0.55 and 0.75).

4.3.2 MODEL CALIBRATION

In situ LAI measurements have been used for producing LAI maps from Landsat-8 and RapidEye images by applying the semi-empirical method by using VIs, the relationship between the WDVI and LAI. Field non-destructive measurements of LAI and leaf mean tilt angle (MTA) were made with LICOR LAI-2000 Plant Canopy Analyzer, which works by comparing the intensity of diffuse incident illumination measured at the bottom of the canopy with that arriving at the top. For reducing the effect of multiple scattering on LAI-2000 measurements, the instrument was only operated near dusk and dawn (6:30-9:30am; 6:30-8:30pm) under diffuse radiation condition using one sensor for both above and below stand measurements. In order to prevent interference caused by the operator's presence and the illumination condition, the sensor field of view was limited with a 180° view-cap. Measurements were azimuthally oriented opposite to the sun azimuth angle. LAI measurements were taken with the instrument held a few centimeters above the soil, generally within 3 days of image data acquisition. One measurement of ambient light was made with the sensor extended upward and over the top of the canopy at arm's length. Eight below-canopy readings were then made. This pattern was repeated three times per spot, and the resulting 24 samples comprise one full set of measurements. Finally, each centre of the LAI-2000 transects were geolocated by using GPS measurements. This protocol ensure a low standard error of measurement to assure 90% to 95% confidence interval. Detail of LAI measurement are reported in Annex 2, while the

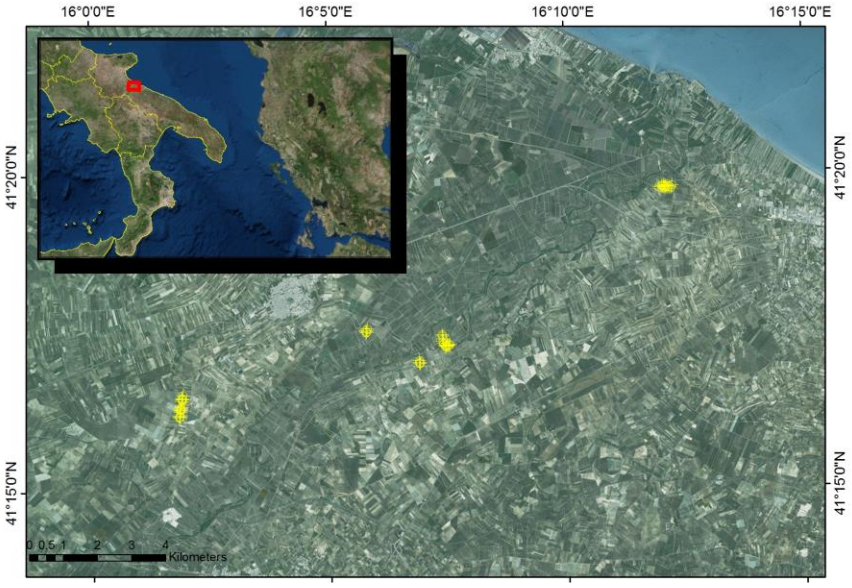

FIGURE 13 - FIELD MEASUREMENTS OF LEAF AREA INDEX (LAI)

following figure shows the location of the LAI measurements..

The CLAIR model needs to be calibrated by estimating the extinction coefficient α*. The equation 5 must be inverted, fixing LAI, WDVI and WDVI∞ values. Thus WDVI values were computed from the pixels of the nearest to RapidEye image in correspondence of LAI measurements. WDVI∞ was calculated (ρi/ρr = 1.35, WDVI∞ = 0.55) as the highest WDVI value of the vegetative areas of the image. The resulted α* values was in the range 0.34 - 0.70. The final value of α*=0.39 was taken in correspondence of the minimum error between observed and estimated LAI, leading to an average error of 25% in the estimation of the LAI.

To quantify the model prediction accuracies root-mean-square error (RMSE) and the coefficient of determination (R^2) between measured and predicted LAI is used (Figure 5). A value of α * '0.39' (R2 = 0.71, RMSE=0.33) have be found taking in account those correlation.

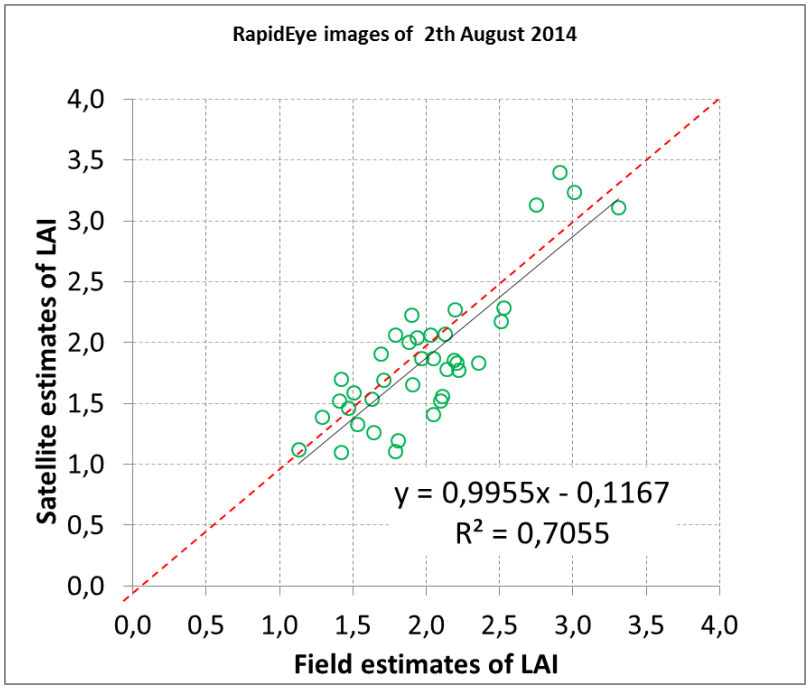

FIGURE 14 - LEAF AREA INDEX (LAI) ESTIMATED (Y) VERSUS LAI MEASURED (X)

4.3.3 Surface Albedo (r) or Spectrally integrated hemispherical reflectance: Theoretical background

The albedo (*r*) can be calculated in different ways (from empirical to physical based approaches). The standard approach is based on empirical broadband coefficients, which are applied to the spectral radiance measured by each channel of the satellite sensor (D'Urso & Belmonte, 2006). Hereby three main problems arise: the directional integration of the spectral radiance detected by the sensor, the spectral integration for obtaining the planetary albedo (albedo of the top of atmosphere - TOA) and the correction of atmospheric effects to achieve the surface albedo (for more details see D'Urso & Belmonte, 2006). So, in IRMA project, the calculation of *r* has been simplified in the following way:

$$r=\Sigma_{\lambda} w_{\lambda} \cdot \rho_{\lambda} \qquad \lambda=1, 2, \ldots, n \tag{9}$$

where ρ_{λ} presents spectral reflectance (corrected for atmospheric effects) in the corresponding band (D'Urso & Belmonte, 2006; Menenti et al., 1989).

Coefficients *w* have been calculated for Landsat 8 OLI, as shown in Table 4.

TABLE 4 - WEIGHTING COEFFICIENTS FOR THE CALCULATION OF ALBEDO (R) BY USING EQ. (9) AND SURFACE REFLECTANCE DERIVED FROM LANDSAT 8 OLI

Sensor & band	E°_{λ} [mW/cm^2 nm]	w_{λ}
Landsat 8 OLI 1	186.311	0.2163
Landsat 8 OLI 2	202.916	0.2356
Landsat 8 OLI 3	188.115	0.2184
Landsat 8 OLI 4	156.339	0.1815
Landsat 8 OLI 5	95.144	0.1105
Landsat 8 OLI 6	24.395	0.0283
Landsat 8 OLI 7	8.200	0.0095

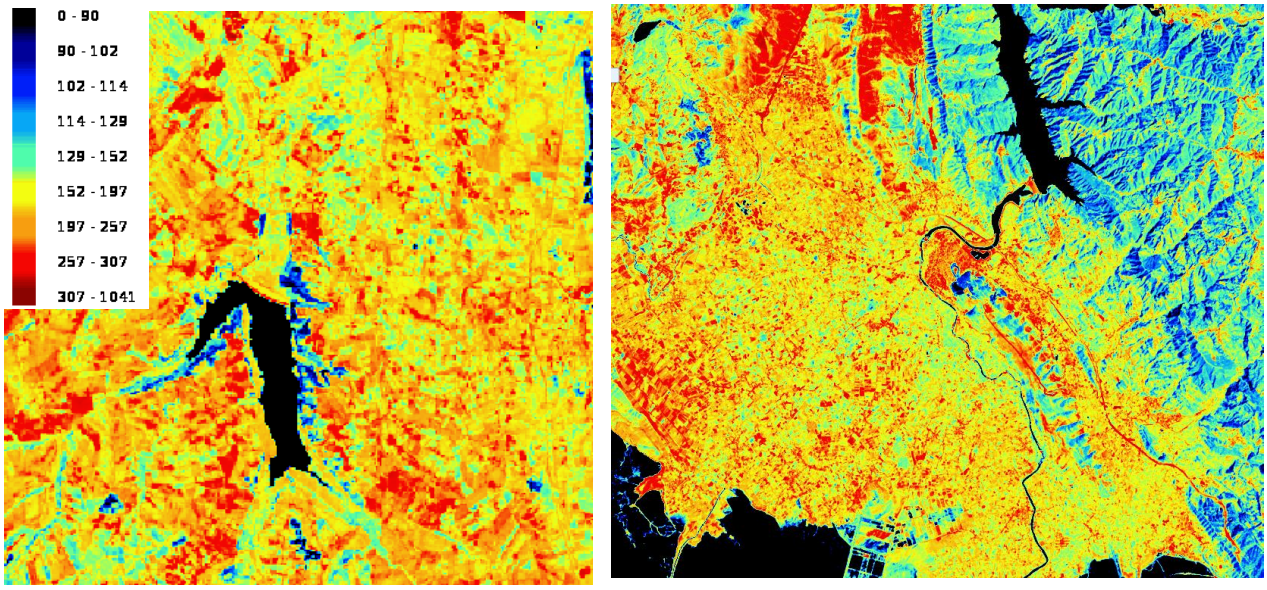

FIGURE 15 - ALBEDO MAPS FOR LANDSAT 8 OLI. A) ITALY DATE 10/08/2014. B) GREECE DATE 05/08/2014

Another way is to derive the ground albedo, the ground reflectance integrated over the wavelength region 0.3 – 2.5 µm. as value adding product from ATCOR (Add-On Module to Intergraph's IMAGINE). The values of albedo derived from ATCOR are free from atmospheric effects and closer to those shown in Table 5

TABEL 5 - SAMPLE ALBEDOS

Surface	Features	Typical Albedo
Soil	Dark and damp	0.05
	Clear and dry	0.4
Sand		0.15-0.45
Lawn		0.16-0.26
Agricultural crops		0.18-0.25
Forest	Decidua	0.15-0.2
	Conifers	0.05-0.15
Water	Low zenith angle	0.03-0.1
	High zenith angle	0.1-1
Snow	Old	0.4
	Fresh	0.95
Cloud	Dense	0.3-0.5
	Thin	0.3-0.5

4.3.4 EVAPOTRANSPIRATION UNDER STANDARD CONDITIONS (ET_P): THEORETICAL BACKGROUND AND EQUATIONS

Crop evapotranspiration under "standard" conditions (ET_p) is the evapotranspiration from disease-free, well-fertilized crops, grown in large fields, under optimum soil water conditions and achieving full production under the given climatic conditions (FAO, 1998). There are basically two approaches to calculate ETp:

a) direct calculation, or "one-step" approach and
b) the "crop coefficient approach", Kc, defined as the ratio of ET_p by reference evapotranspiration ET_0;

4.3.5 DIRECT CALCULATION OF ETP

Direct calculation of crop evapotranspiration (a) is derived from meteorological and crop data by means of the Penman-Monteith equation (Monteith, 1965).

$$ETo = \frac{8640}{\lambda} \quad \frac{\Delta(R_n - \mathrm{G}) + c_p\ p_a(e_s - e_a)/r_{a,h}}{s + \gamma(1 + r_c/r_{a,h})} \tag{10}$$

with:

ETo crop evapotranspiration (mm/day)
Δ slope of the saturated vapour pressure-temperature curve es(T) (kPa/K)
Rn net solar radiation (W/m^2)
G heat flux density into the soil (W/m^2)
cp air specific heat (J/kg K)
p_a air density (kg/m^3)
es-ea vapor pressure deficit, given by the difference between saturated and actual vapor pressure (kPa) at the given air temperature Ta.
$r_{a,h}$ aerodynamic resistance (s/m), which depends on the wind speed and aerodynamic properties of the surface
r_s surface resistance (s/m)
γ thermodynamic psychrometric constant (kPa/K), and
λ latent heat of vaporisation of water (J/kg).

The formulae for calculating each parameter can be found extensively in 'FAO Irrigation and Drainage paper No. 56' by FAO (1998)

Assuming the standard parameters for the reference of *hc* = 0.12 m, a fixed canopy resistence *rc* = 70 s/m an albedo of *r* = 0.23 and *LAI* = 2.88 m^2/ m^2, eq. 10 can be rewritten as;

$$ETp = \frac{8640}{\lambda} \frac{\Delta(1 - 0.4e^{0.5LAI})[(1 - r)K^+ + L^*] + c_p p_a\ (e_s - e_a)U/124}{[\Delta + \lambda\left(1 + \frac{U}{1.24LAI}\right)]} \tag{11}$$

Where U represent the wind speed (m/s), K^+ is the flux density of incoming short wave radiation (W/m^2) and L* is the net incoming longwave radiation flux density (W/m^2). The constant 8640 in equation (10) implies the use of average daily values for the required meteorological data.

In this equation explicitly compare the crop parameters surface albedo, the Leaf Area Index (LAI) that can be obtained from the processing of satellite images. Regarding the crop eight sensitivity analysis of the value of ETp with respect to these parameters, carried out in the Mediterranean area (characterized by strong solar irradiation conditions) showing that, the value of ETp is more closely related to vegetation parameters r, LAI, and that the sensitivity of the change in the crop height of the ETp is higher in autumn than in summer (D'Urso, 2001).

This is due to the fact that, at the daily scale, the aerodynamic component of evapotranspiration, in the aforementioned weather conditions, is of much less importance than radiative.

Recent studies conducted in semi-arid areas (Aghdasi, 2010), confirms this trend, in fact to a percentage change of 50% in hc corresponds a variation of the order of 5% of ETp. Therefore a constant value of hc = 0.4 m has been set, valid for the climatic conditions of the Mediterranean area, reducing the calculation to the estimation of albedo and LAI (with the methodologies aforementioned).

4.3.6 CROP COEFFICIENT APPROACH

In the FAO crop coefficient approach (b), ET_p is calculated by multiplying reference evapotranspiration (ET_0) with the crop coefficient (Kc):

$$ET_p = Kc \cdot ET_0 \tag{12}$$

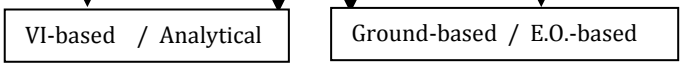

with ET_p and ET_0 in [mm/d] and Kc [dimensionless].

The crop coefficient, Kc is basically the ratio of the crop ETp to the reference ETo, calculated with eq. 10, can be written in the following form (FAO, 1996):

$$K_c = \frac{ETc\left(r^*, LAI^*, hc^*; Ta, RH, U, K^{\downarrow}\right)}{ETo(r, LAI, hc; Ta, RH, U, K^{\downarrow})} \tag{13}$$

Where r*, LAI* (with hc*=0.4) represent the parameters of the crop vegetation present at the time of the satellite overpass, which can be related to satellite observations

The Kc parameter differentiates the physical and physiological characteristics of the crops and can be estimated by analytical approaches as discussed in the previous section. The effects of weather conditions on crop evapotranspiration are described by ET_0.

The canopy parameters (and consequently the Kc value) can be considered as constant for a time period of approx. 5-7 days around the date of the satellite overpass. Diversely, meteorological data are extremely variable. Therefore, Kc-value can be calculated for a short period of time, expressing it as a function of albedo (r) and LAI in a polynomial form:

$$\begin{aligned} K_c(r, LAI) = &\left(a_4 + b_4 \cdot r\right) LAI^4 + \left(a_3 + b_3 \cdot r\right) LAI^3 + \left(a_2 + b_2 \cdot r\right) LAI^2 + \\ &+ \left(a_1 + b_1 \cdot r\right) LAI + \left(a_0 + b_0 \cdot r\right) \end{aligned} \tag{14}$$

where the set of coefficients {a*i*,b*i*} are derived in two steps:

1. by calculating ETp with the daily meteorological data observed during a period of 5-7 days before the date of satellite pass;
2. by averaging out the resulting Kc for each day.

4.3.7 IRRIGATION WATER REQUIREMENTS (IWR)

The irrigation water required by a crop growing under potential conditions is finally calculated as a function of ETp and the precipitation rate (Pn), actually infiltrating through the soil surface (D'Urso, 2001):

$$IWR = ET_p - P_n \quad (14)$$

In order to describe the amount of intercepted (precipitation and irrigation) water from plant surface, Pn is calculated as a function of the actual precipitation (P), LAI and fractional cover (fc). The semi-empirical model of interception (Braden, 1985, D'Urso, 2001), implemented into the SIMODIS model (D'Urso, 2001), describes this relationship as follows:

$$P_n = P - aLAI\left(1 - \frac{1}{1 + \frac{f\text{cover} \cdot P}{aLAI}}\right) \quad (15)$$

with P in (mm/d), and α in (cm/d), being an empirical parameter representing the crop saturation per unit foliage area (~0.28 for most crops).

4.4 IMAGES CLASSIFICATION

Satellite images were classified to identify during the time (2013 and 2014) the two classes:

- agricultural field with vegetation
- bare soil and/or urban areas.

In this study it was used the "supervised" classification. It start from an initial identification of certain areas or pixels from the image that are known (training pixel) at the two classes. These pixels are very homogeneous and spectrally distinct. The software then attempts to assign the remaining pixels to the most similar training class.

A classification was made for each satellite images (single-date), because the classification results are notoriously sensitive to changing atmospheric conditions, use of different sensors and time of year of image acquisition.

4.5 EVAPOTRANSPIRATION MAPS

The total amount of Crop Water Requirement (CWR= ETp) maps were elaborated with decadal times following several steps. For year 2013 and 2014, in every study area, all Landsat satellite images were elaborated and it was calculated the crop coefficient map. The crop coefficient maps generated for each satellite images are processed to identify areas cultivated (i.e., excluding areas devoid of vegetation, urban centers, roads). This allowed to estimate, on a decade basis, the crop water requirements of the irrigation districts present in the area of study.

The irrigated area was calculated as the area with kc >0.4. Then the ETp maps were created by the relation ETp=Kc*ETo. The map of total evapotranspiration was created as the sum of the decadal ETp maps.

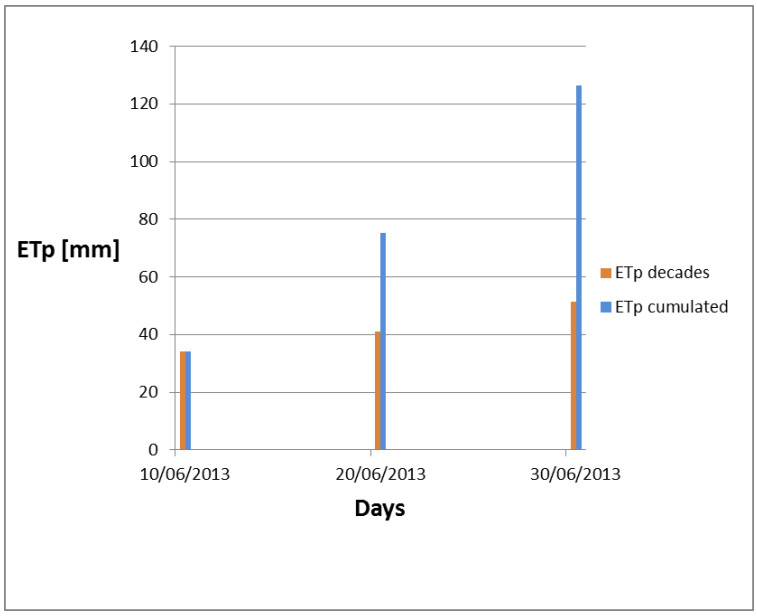

FIGURE 16 - EXAMPLE OF ETP CUMULATED IN AN AREA

5. RESULTS

In this study, satellite images of two different sensor were analyzed and the images elaborated are depict in Table 6. (Detailed result will be object of scientific publication).

TABLE 6 - MAPS DERIVED FROM SATELLITE IMAGES DIVIDED BY AREA

Num. total	Map description	Italian study area	Greece study area
50	Georeferenced maps	37	13
50	Surface reflectance calibrated maps	37	13
50	Ground albedo maps	37	13
50	NDVI maps	37	13
50	WDVI	37	13
50	LAI maps	37	13
37	Soil cover	24	13
50	Crop coefficient (Kc) maps	37	13
50	Classified maps	37	13
43	ETp maps	32	11
43	Total Irrigated Water Requirement (IWR)	32	11
41	Decades IWR	22	19
35	Classified maps	24	11
3	CWR (or ETp) cumulated maps	2 (2013 and 2014)	1 (2013)

The total amount of CWR (=ETp) in the two study area is described in table 7: one part of water is discharged by water stock in the soil, one part from precipitations and the remain from irrigation.

TABLE 7 - RIEPILOGO DEI DATI STATISTICI PER LE MAPPE DI EVAPORAZIONE CUMULATE PRODOTTE PER STAGIONE IRRIGUA E PER AREA DI STUDIO

Study area	Year	CWR [mm/ha]		
		max	mean	Std.Dev
Apulia	2013	569	179	136
	2014	1127	406	168
Grecee	2013	623	390	102

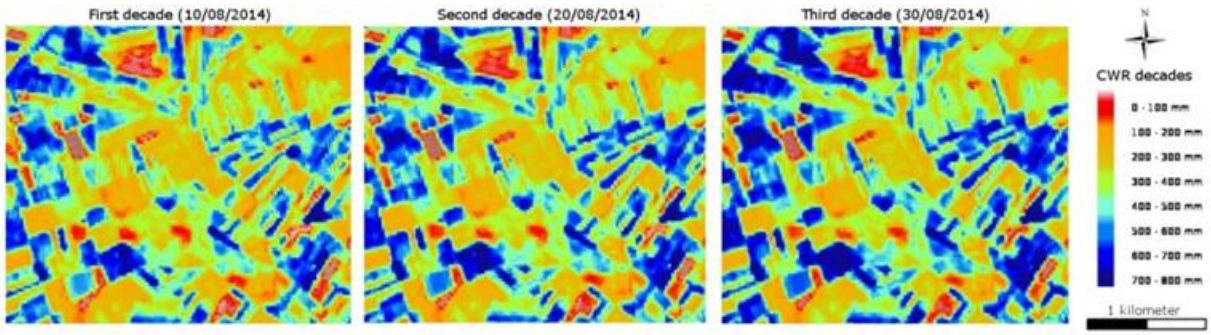

FIGURE 17 -CWR MAPS IN THE STUDY AREA AVAILABLE IN WEB-GIS SYSTEM.

6. VALIDATION

The validation procedure is performed at two different levels:

- accuracy estimation of canopy parameters based on field measurements (**Errore. L'origine riferimento non è stata trovata.**see annex 2)
- comparison between suggested and actually applied irrigation volumes, at farm level.

The first level of validation is performed in coincidence of the satellite acquisition in selected plot with different crops. A portable LAI digital meter (Licor LAI-2000) is used to measure the value of LAI in the field; successively, this georeferenced measurement is compared with the value resulting in the LAI map derived by analyzing the satellite image.

The second level of validation it will be possible with availability of irrigation applications at farm level. With automatic registrations of water withdrawals from the distribution network are available it will be possible to evaluate the correspondence between the volumes indicated by IRMA and those applied by the Irrigation District.

To validate the estimation of LAI from satellite data, measurements of canopy transmittance were taken in 44 Italian sites (Table 3) during a field campaign in July 2014, the positions of these sites were recorded with GPS. In a GIS environment a map with plot was digitalized to extract the kc of different parcels. The field measurement protocol was designed to ensure a consistent and repeatable set of measurements in each vineyard within the study area.

LAI was estimated using the Plant Canopy Analyzer LAI-2000 (LI-COR, 1992). Data acquisition included replicate measurements of incident radiation both above and below the canopy. Measurements were made during early morning and late afternoon under diffuse light conditions to minimize the effects of direct sunlight otherwise leading to LAI underestimation. To quantify the model prediction accuracies we used the following statistical measures: RMSE, the coefficient of determination (R2) between measured and predicted LAI and the confidence intervals.

7. WEB-GIS

The maps and suggested irrigation volume applications are timely published on a dedicated webGIS-site (http://95.110.192.55/irma/),in order to better control the irrigation process and consequently improve its overall efficiency.

An intuitive web-interface has been developed to give growers also the ability to monitor the canopy development at plot level in near-real time and the evaluation of net precipitation, thanks to a better calculation of canopy interception based from satellite LAI values may reduce the irrigation application.

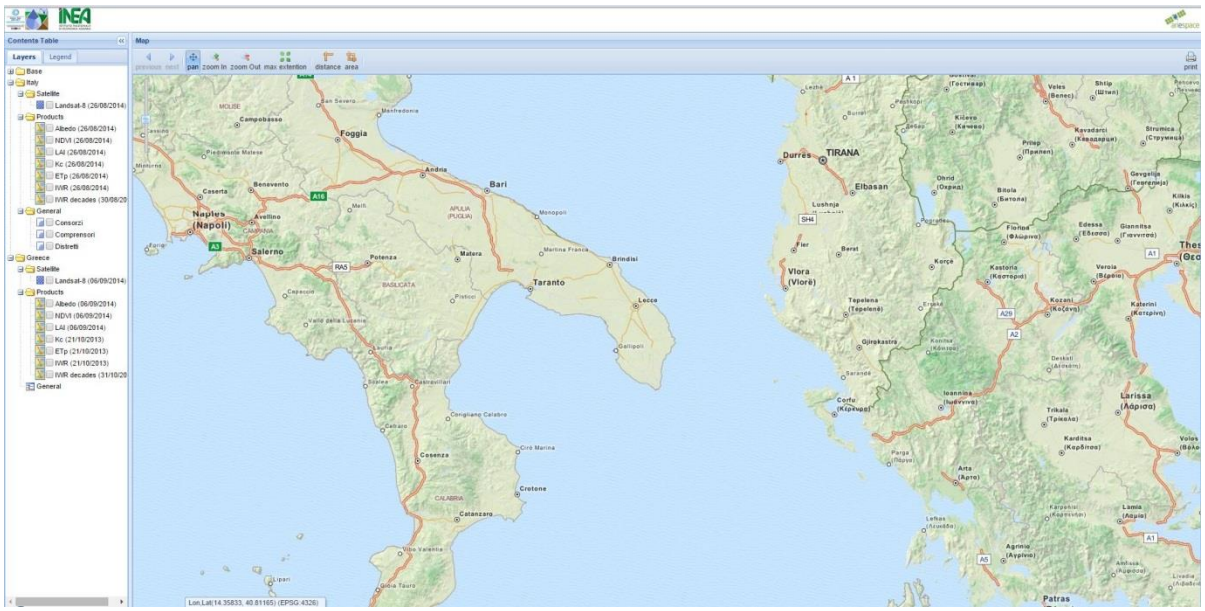

FIGURE 18 - IRMA IRRIGATION MANAGEMENT: MAIN PAGE

The irrigation volume is calculated by using the LAI and albedo maps (derived from satellite data) , the potential ETp and effective rainfall Data refer to a period of approx. 7 days; results are expressed in mm/day; mm/decades.

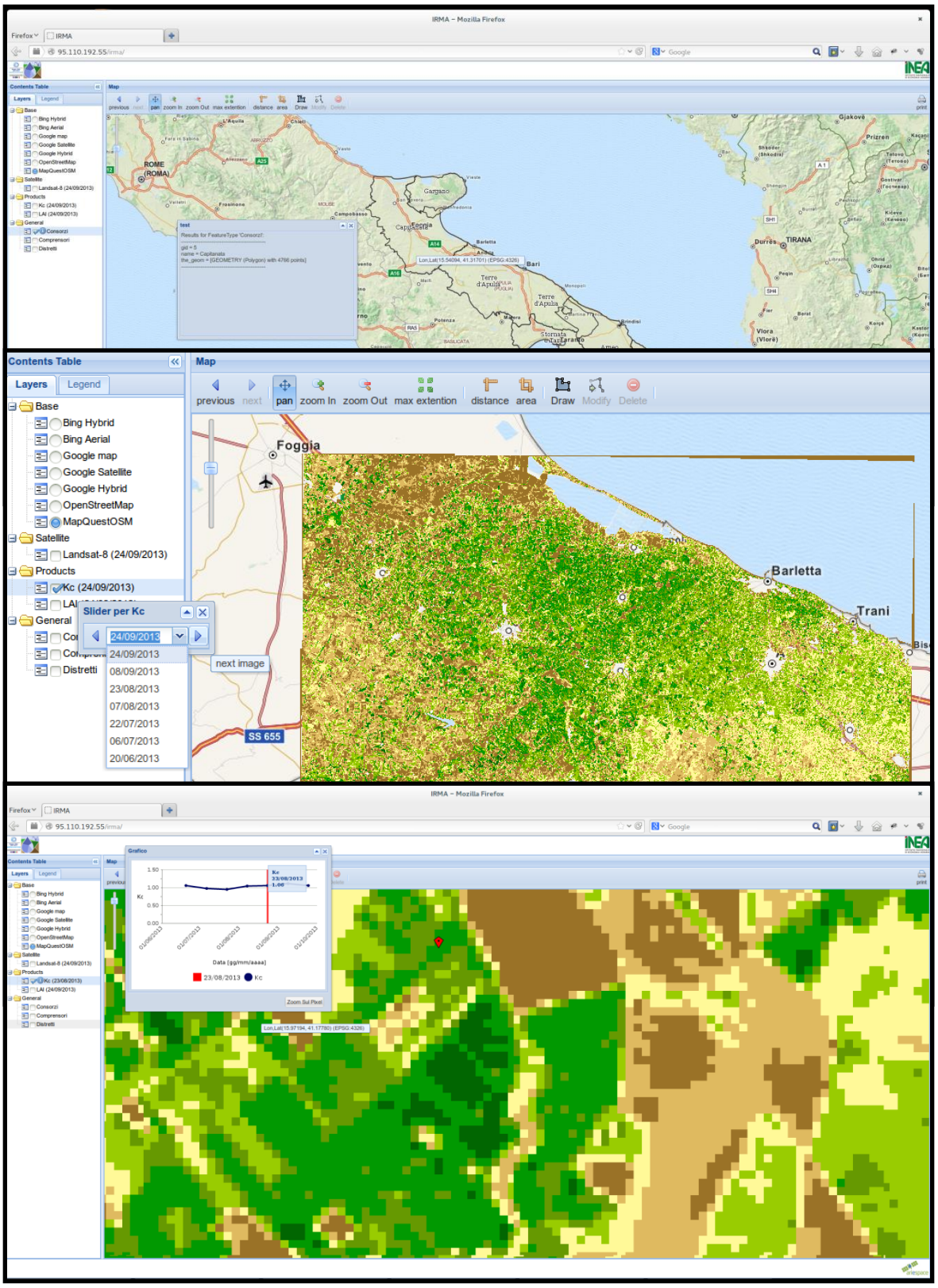

FIGURE 19 - QUERY DATA FRAME: TABLE AND GRAPHS

8. LANDSCAPE ASPECTS

To evaluate evapotranspiration in the landscape area, the following steps were done:

- digitalization of landscape objects (recreational fields - golf, soccer, tennis.- public parks, etc) with photointerpretation of Google maps presents in the two study areas (Italy and Greece);
- acquisition of other satellite images respect those collected to analysed agricultural areas for 2013 and 2014;
- elaboration of satellite images with the methodology described previously for the landscape areas earlier described.

The following section report the results obtained in the study area.

8.1 GREECE STUDY AREA

A total number of 37 item of different landscape have been identified, locates as reported in the following table.

TABLE 8 –LOCATION OF LANDSCAPE IDENTIFIED IN GREECE STUDY AREA

Name	Area	Municipality	Name	Area	Municipality
Skopeftirio FB field	Arta	Arta	Tennis Club	Arta	Arta
AnAnargyroi FB field	Agioi Anargyroi	Arta	Parapotamio Park	Arta	Arta
Kostakii FB field	Kostakii	Arta	Peta	Peta	N. Skoufa
Keramates FB field	Keramates	Arta	Megarxis	Magarxi	N. Skoufa
Keramates 5x5 FB field	Keramates	Arta	Selladon 5x5	Sellades	N. Skoufa
Arta FB Stadium	Arta	Arta	Selladon	Sellades	N. Skoufa
Glykorizou	Arta	Arta	Kompotiou	Kompoti	N. Skoufa
Korfovouniou	Korfovouni	Arta	Pahikalamou	Pahikalamos	N. Skoufa
Grammenitsas	Grammenitsa	Arta	Akropotamias	Akropotamia	N. Skoufa
Hanopoulou	Gribovo	Arta	Neohoriou	Neohori	N. Skoufa
Kalamias	Kalamia	Arta	Loutrotopou	Loutrotopos	N. Skoufa
Kampis	Kampi	Arta	Agias Paraskeyis	Agia Paraskeyi	N. Skoufa
Rokka	Rokka	Arta	Vlaxerna	Valxerna	Arta
Filotheis	Filothei	Arta	Gavrias	Gavria	Arta
Kalovatou	Kalovatos	Arta	Strogylis	Strogyli	Arta
Plision	Kirikizates	Arta	Agiou Spiridona	Agios Spyridon	Arta
Kalogerikou	Kalogeriko	Arta	Rahis	Rahi	Arta
Anezas	Aneza	Arta	Viglas	Vigla	Arta
Polydrosou	Polydroso	Arta			

The total area of the urban landscape is around 103 ha, while the total CWR is 89,600 mm/year, with an average value of 868 mm/ha/year.

8.2 ITALY STUDY AREA

A total number of 122 item of different landscape have been identified, locates as reported in the following tables.

TABLE 9-URBAN LANDSCAPE: TARGET " FOOTBALL FIELD"

N° progressivo	nome	estensione [Ha]
1	viale_europa	0.4
2	di_cagno	0.4
3	campo_polisportivo_nicola_rossiello	0.5
4	di_cagno	0.5
5	passe_partout	0.5
6	fanelli	0.5
7	via_chieti	0.6
8	leo_dell'acqua	0.6
9	complesso_sportivo_tonino_rana	0.6
10	stadio_madonna_d'altomare	0.7
11	campo_comunale_di_palese	0.7
12	campo_dei_fiori	0.7
13	campo_comunale_antonio_antonucci	0.7
14	campo_comunale_tommaso_carrieri	0.7
15	francesco_capocasale	0.7
16	complesso_sportivo_tonino_rana	0.8
17	campo_comunale_città_degli_ulivi_bitonto	0.8
18	campo_via_dello_stadio	0.8
19	torrebella	0.8
20	noicattaro	0.8
21	san_nicola	0.8
22	sante_diomede	0.8
23	arena_della_vittoria	0.9
24	campo_sportivo_mirko_variato	0.9
25	stadio_comunale_vito_curlo	0.9
26	passe_partout	0.9
27	via_chieti	1.0
28	via_togliatti	1.0
29	sigismondo_palmiotta	1.0
30	campo_comunale_capurso	1.1
31	campo_comunale_rutigliano	1.3
32	campo_polisportivo_nicola_rossiello	1.4
33	campo_ostuni	1.7
34	campo_comunale_giammaria	1.9
35	campo_comunale_di_valenzano	2.2
36	campo_comunale_scianni_ruggieri	2.5
37	campo_sportivo_comunale_san_pio	3.0
38	campo_comunale_peppino_lorusso	3.2
39	campo_polisportivo_via_grumo	3.8
40	stadio_via_del_mare	20.5
	TOT	***63.8***

TABLE 10 - URBAN LANDSCAPE: TARGET " PUBLIC PARK"

N° progressivo	nome	estensione [Ha]
1	area_verde_via_brubelleschi	0.4
2	piaza_due_giugno	0.4
3	piazza_ludovico_ariosto	0.4
4	area_verde_via_della_vittoria	0.4
5	piazza_zanardelli	0.4
6	area_verde_via_albanese	0.5
7	pineta_comunale_bitetto	0.5
8	area_municipio_valenzano	0.5
9	piazza_italia_lecce	0.6
10	piazza_vittorio_emanuele_II	0.6
11	area_verde_via_falconieri	0.6
12	piazza_vittorio_emanuele_II	0.7
13	area_verde_via_carducci	0.7
14	piazza_giovanni_XXIII	0.7
15	area_verde_via_dei_trulli	0.7
16	parco_della_rimembranza	0.8
17	area_verde_via_da_vinci	0.9
18	villa_garibaldi	0.9
19	area_verde_via_della_vittoria	1.0
20	area_verde_strada_provinciale_144	1.0
21	piazza_mazzini	1.2
22	villa_comunale_altamura	1.2
23	piazza_umberto_I	1.2
24	area_verde_via_XXIV_maggio	1.2
25	area_verde_via_avellino	1.3
26	piazza_garibaldi	1.4
27	villa_carmine	1.4
28	parco_urbano_capurso	1.5
29	area_verde_via_corvaglia	1.5
30	piazza_garibaldi	1.5
31	villa_comunale_mesagne	1.6
32	pineta_san_paolo	1.7
33	parco_rimembranze	1.7
34	piazza_antonio_gramsci	2.0
35	piazza_umberto_I	2.1
36	area_verde_via_firenze	2.4
37	giardino_peppino_impastato	2.5
38	francavilla_fontana	2.9
39	villa_comunale_giovanni_XXIII	3.3
40	giardini_pubblici_lecce	3.6
41	parco_padre_pio	3.6
42	area_verde_via_san_gaspare_del_bufalo	3.8
43	area_verde_via_XX_settembre	4.9
44	villa_reale_lecce	5.0
45	parco_perotti	5.2
46	parco_comunale_cesare_braico	6.0
47	parco_due_giugno	6.2
48	chiesa_san_pietro_mandurino	6.9
49	parco_tre_ponti	7.0
50	pineta_san_francesco	7.7
51	area_verde_via_della_cavalleria	9.4
52	parco_archeologico_mura_messapiche	15.6
53	parco_naturale_regionale_lama_balice	192.6
54	riserva_statale_lago_di_lesina	1097.4
55	parco_naturale_bosco_incoronata	1820.5
56	bosco_difesa_grande_di_gravina	2184.7
57	parco_nazionale_alta_murgia	68645.2
	TOT	***74071.2***

TABLE 11- URBAN LANDSCAPE: TARGET "TENNIS FIELD"

N° progressivo	nome	estensione [Ha]
1	country_club	0.1
2	frattasi	0.1
3	country_club	0.1
4	frattasi	0.1
5	frattasi	0.1
6	frattasi	0.1
7	country_club	0.1
8	frattasi	0.1
9	country_club	0.1
10	campo_polisportivo_via_grumo	0.1
11	circolo_tennis	0.1
12	circolo_tennis	0.1
13	bonomo	0.1
14	frattasi	0.1
15	campo_sportivo_mirko_variato	0.1
16	frattasi	0.1
17	frattasi	0.1
18	circolo_tennis_triggiano	0.2
19	bonomo	0.2
20	bonomo	0.3
	TOT	2.6

TABELLA 12 - TABLE 11- URBAN LANDSCAPE: TARGET "GOLF FIELD"

N° progressivo	nome	estensione [Ha]
1	san_domenico	68.2
2	bari_alto	49.4
3	doubletree	108.9
4	riva_dei_tessali	404.7
5	masseria_torre_coccaro	6.9
	TOT	638.1

The total area of the urban landscape is around 74,776 ha, while the total CWR is around 50,250,000 mm/year with an average value of 672 mm/ha/year.

Detailed result will be object of scientific publication.

9. REFERENCES

Allen RG, Pereira LS, Raes D, Smith M (1998) Crop evapotranspiration: Guidelines for computing crop requirements. Irrigation and Drainage Paper No. 56, FAO, Rome, Italy.

Breda, N.J.J. (2003). Ground-based measurements of leaf area index: a review of methods, instruments and current controversies. Journal of Experimental Botany 54(392), 2403-2417.

Chander G, Markham B, Helder L (2009) Summary of current radiometric calibration coefficients for Landsat MSS, TM, ETM+, and EO-1 ALI sensors. Remote Sensing of Environment 113, 893-903.

Chen X, Vierling L, Deering D (2005) A simple and effective radiometric correction method to improve landscape change detection across sensors and across time. Remote Sensing of Environment 98, 63-79.

Clevers, J. G. P. W., 1989. The application of a weighted infrared-red vegetation index for estimating leaf area index by correcting for soil moisture. *Remote Sens. Environ.*

D'Urso, G. (2001): Simulation and management of on-demand irrigation systems: a combined agrohydrological and remote sensing approach (PhD thesis) Wageningen Agricultural University, 173 pp.

D'Urso, G., Calera Belmonte, A (2006): Operative approaches to determine crop water requirements from Earth Observation data: methodologies and applications. AIP conference proceedings 852: Earth Observation for Vegetation and Water Management, pp. 14-25, 2006.

Hagolle O, Huc. M, Villa Pacula D, Dedieu G (2010) A multi-temporal method for cloud detection, applied to FORMOSAT-2, VENS, LANDSAT and SENTINEL-2 images. Remote Sensing of Environment 114, 1747-1755.

LI-COR, 1992. LAI-2000 plant canopy analyzer instruction manual.

Lyapustin A, Wang Y, Frey R (2008) An automatic cloud mask algorithm based on time series of MODIS measurements. Journal of Geophysical Research 113, D16207, 15 Pages.

Martínez-Beltrán C, Osann Jochum MA, Calera A, Meliá J (2009) Multisensor comparison of NDVI for a semi-arid environment in Spain. International Journal of Remote Sensing 30, 1355-1384.

Monteith J.L., Evaporation and environment. In: The state and movement of water in living organism. 19th Symp Soc Exp Biol. 1965;19:205-34.

Monteith, J. L., 1977, Climate and the efficiency of crop production in Britain, Phil. Trans. R. Soc. London B281: 277-294.

Schroeder TA, Cohen WB, Song C, Canty MJ, Yang Z (2006) Radiometric correction of multi-temporal Landsat data for characterization of early successional forest patterns in western Oregon. Remote Sensing of Environment 103, 16-26.

Steven MD, Malthus TJ, Baret F, Xu H, Chopping MJ (2003) Intercalibration of vegetation indices from different sensors system. Remote Sensing of Environment 88, 412-422.

ANNEX 1

DETAIL ON IMAGES AQUISITION

TABLE 13 - LANDSAT 8 OLI - PUGLIA ITALY

Number	path	row	Data	ID image	Folder	data type level	image quality
1	188	31	19/5/2013	LC81880312013139LGN01	20130519_lt8_31	LT1	9
2	188	32	19/5/2013	LC81880322013139LGN01	20130519_lt8_32	LT1	9
3	188	31	20/6/2013	LC81880312013171LGN00	20130620_lt8_31	LT1	9
4	188	32	20/6/2013	LC81880322013171LGN00	20130620_lt8_32	LT1	9
5	188	31	6/7/2013	LC81880312013187LGN00	20130706_lt8_31	LT1	9
6	188	32	6/7/2013	LC81880322013187LGN00	20130706_lt8_32	LT1	9
7	188	31	22/7/2013	LC81880312013203LGN00	20130722_lt8_31	LT1	9
8	188	32	22/7/2013	LC81880322013203LGN00	20130722_lt8_32	LT1	9
9	188	31	7/8/2013	LC81880312013219LGN00	20130807_lt8_31	LT1	9
10	188	32	7/8/2013	LC81880322013219LGN00	20130807_lt8_32	LT1	9
11	188	31	23/8/2013	LC81880312013235LGN00	20130823_lt8_31	LT1	9
12	188	32	23/8/2013	LC81880322013235LGN00	20130823_lt8_32	LT1	9
13	188	31	8/9/2013	LC81880312013251LGN00	20130908_lt8_31	LT1	9
14	188	32	8/9/2013	LC81880322013251LGN00	20130908_lt8_32	LT1	9
15	188	31	24/9/2013	LC81880312013267LGN00	20130924_lt8_31	LT1	9
16	188	32	24/9/2013	LC81880322013267LGN00	20130924_lt8_32	LT1	9
17	188	31	10/10/2013	LC81880312013283LGN00	20131010_lt8_31	LT1	9
18	188	32	10/10/2013	LC81880322013283LGN00	20131010_lt8_32	LT1	9
19	188	31	26/10/2013	LC81880312013299LGN00	20131026_lt8_31	LT1	9
20	188	32	26/10/2013	LC81880322013299LGN00	20131026_lt8_32	LT1	9
21	188	31	13/12/2013	LC81880312013347LGN00	20131213_lt8_31	LT1	9

22	188	32	13/12/2013	LC81880322013347LGN00	20131010_lt8_32	LT1	9
23	188	31	29/12/2013	LC81880312013363LGN00	20131026_lt8_31	LT1	9
24	188	32	29/12/2013	LC81880322013363LGN00	20131026_lt8_32	LT1	9
25	188	31	14/01/2014	LC81880312014014LGN00	20131213_lt8_31	LT1	9
26	188	32	14/01/2014	LC81880322014014LGN00	20131213_lt8_32	LT1	9
27	188	31	15/02/2014	LC81880312014046LGN00	20131229_lt8_31	LT1	9
28	188	32	15/02/2014	LC81880322014046LGN00	20131229_lt8_32	LT1	9
29	188	31	19/03/2014	LC81880312014078LGN00	20140114_lt8_31	LT1	9
30	188	32	19/03/2014	LC81880322014078LGN00	20140114_lt8_32	LT1	9
31	188	31	06/05/2014	LC81880312014126LGN00	20140215_lt8_31	LT1	9
32	188	32	06/05/2014	LC81880322014126LGN00	20140215_lt8_32	LT1	9
33	188	31	07/06/2014	LC81880312014158LGN00	20140319_lt8_31	LT1	9
34	188	32	07/06/2014	LC81880322014158LGN00	20140319_lt8_32	LT1	9
35	188	31	23/06/2014	LC81880312014174LGN00	20140506_lt8_31	LT1	9
36	188	32	23/06/2014	LC81880322014174LGN00	20140506_lt8_32	LT1	9
37	188	31	09/07/2014	LC81880312014190LGN00	20140607_lt8_31	LT1	9
38	188	32	09/07/2014	LC81880322014190LGN00	20140607_lt8_32	LT1	9
39	188	31	10/08/2014	LC81880312014222LGN00	20140623_lt8_31	LT1	9
40	188	32	10/08/2014	LC81880322014222LGN00	20140623_lt8_32	LT1	9
41	188	31	26/08/2014	LC81880312014238LGN00	20140709_lt8_31	LT1	9
42	188	32	26/08/2014	LC81880322014238LGN00	20140709_lt8_32	LT1	9

TABLE 14 - RAPID-EYE - PUGLIA ITALY

Number	Data	ID image	Folder	data type level
1	21/06/2013	2013-06-21T104513_RE2_1B-NAC_13078218_164046	20130621_re	RE2-1B
2	10/06/2014	2014-06-10T105014_RE3_1B-NAC_16659721_180267	20140610_re	RE2-1B
3	11/06/2014	2014-06-11T103340_RE5_1B-NAC_16685960_180267	20140611_re	RE2-1B
4	16/07/2014	2014-07-16T105020_RE1_1B-NAC_17115301_195108	20140716_re	RE2-1B
5	02/08/2014	2014-08-02T104332_RE4_1B-NAC_17325931_195108	20140802_re	RE2-1B
6	04/08/2014	2014-08-04T105030_RE1_1B-NAC_17363833_211196	20140804_re	RE2-1B
7	08/08/2014	2014-08-08T105157_RE5_1B-NAC_17403666_195108	20140808_re	RE2-1B
8	30/08/2014	2014-08-30T103304_RE4_1B-NAC_17649045_214451	20140830_re	RE2-1B
9	08/09/2014	2014-09-08T104242_RE3_1B-NAC_17764601_214451	20140908_re	RE2-1B
10	09/09/2014	2014-09-09T104300_RE4_1B-NAC_17780181_221511	20140909_re	RE2-1B
11	29/09/2014	2014-09-29T104558_RE5_1B-NAC_18017732_221511	20140929_re	RE2-1B

TABLE 15- RAPIDEYE AND RELATED MOSAIC - PUGLIA ITALY

N°	Satellite	Date of acquisition	Date image mosaic
1	RapidEye	21/06/2013	21/06/2013
2	RapidEye	10/06/2014	10/06/2014
3	RapidEye	11/06/2014	
4	RapidEye	16/07/2014	16/07/2014
5	RapidEye	02/08/2014	05/08/2014
6	RapidEye	04/08/2014	
7	RapidEye	08/08/2014	
8	RapidEye	30/08/2014	04/09/2014
9	RapidEye	08/09/2014	
10	RapidEye	09/09/2014	
11	RapidEye	29/09/2014	29/09/2014

TABELLA 16 - LANDSAT 8 OLI - GREECE

Number	path	row	Data	ID image	Folder	data type level	image quality
1	185	33	12/4/2013	LC81850332013102LGN01	20130412_lt8_33	LT1	9
2	185	33	28/4/2013	LC81850332013118LGN01	20130428_lt8_33	LT1	9
3	185	33	14/5/2013	LC81850332013134LGN01	20130514_lt8_33	LT1	9
4	185	33	30/5/2013	LC81850332013150LGN00	20130530_lt8_33	LT1	9
5	185	33	15/6/2013	LC81850332013166LGN00	20130615_lt8_33	LT1	9
6	185	33	1/7/2013	LC81850332013182LGN00	20130701_lt8_33	LT1	9
7	185	33	2/8/2013	LC81850332013214LGN00	20130802_lt8_33	LT1	9
8	185	33	18/8/2013	LC81850332013230LGN00	20130818_lt8_33	LT1	9
9	185	33	3/9/2013	LC81850332013246LGN00	20130903_lt8_33	LT1	9
10	185	33	19/9/2013	LC81850332013262LGN00	20130919_lt8_33	LT1	9
11	185	33	05/10/2013	LC81850332013278LGN00	20131005_lt8_33	LT1	9
12	185	33	21/10/2013	LC81850332013294LGN00	20131021_lt8_33	LT1	9
13	185	33	08/12/2013	LC81850332013342LGN00	20131208_lt8_33	LT1	9
14	185	33	09/01/2014	LC81850332014009LGN00	20140109_lt8_33	LT1	9
15	185	33	14/03/2014	LC81850332014073LGN00	20140314_lt8_33	LT1	9
16	185	33	30/03/2014	LC81850332014089LGN00	20140330_lt8_33	LT1	9
17	185	33	04/07/2014	LC81850332014185LGN00	20140704_lt8_33	LT1	9
18	185	33	20/07/2014	LC81850332014201LGN00	20140720_lt8_33	LT1	9
19	185	33	05/08/2014	LC81850332014217LGN00	20140805_lt8_33	LT1	9
20	185	33	21/08/2014	LC81850332014233LGN00	20140821_lt8_33	LT1	9
21	185	33	06/09/2014	LC81850332014249LGN00	20140906_lt8_33	LT1	9

TABELLA 17 - RAPID-EYE – GREECE

Number	Data	ID image	Folder	data type level
1	12/06/2014	2014-06-12T101829_RE2_1B-NAC_16692959_182378	20140612_re	RE2-1B
2	22/07/2014	2014-07-22T101326_RE4_1B-NAC_17193039_182378	20140722_re	RE2-1B

ANNEX 2

DETAIL ON LEAF AREA INDEX MEASUREMENT

TABLE 18 - FIELD MEASUREMENTS OF LEAF AREA INDEX (LAI)

Num_file	What	LAI	Lat	Long
18	Vineyard	1,79	41,2915	16,0964
19	Vineyard	2,11	41,2919	16,0962
20	Vineyard	2,15	41,2919	16,0963
21	Vineyard	1,29	41,2708	16,0308
22	Vineyard	2,05	41,269603	16,030604
24	Peach	3,39	41,26947	16,030323
25	Vineyard	1,69	41,271438	16,030842
26	Vineyard	1,97	41,271528	16,031182
27	Vineyard	2,05	41,271573	16,030798
28	Vineyard	1,13	41,271808	16,030914
29	Vineyard	1,88	41,272141	16,031001
30	Vineyard	1,42	41,269764	16,030566
31	Vineyard	2,45	41,274512	16,031439
32	Peach	3,31	41,274272	13,031563
33	Vineyard	2,91	41,274235	16,03137
34	Vineyard	2,4	41,273756	16,031573
35	Peach	2,75	41,274097	16,031535
36	Vineyard	3,01	41,275297	16,031716
37	Vineyard	1,91	41,328946	16,201874
38	Vineyard	1,94	41,32873	16,201479
39	Vineyard	1,47	41,329017	16,202431
40	Vineyard	1,53	41,329046	16,203089
41	Vineyard	1,81	41,328733	16,203716
42	Vineyard	1,42	41,329335	16,204028
43	Vineyard	1,63	41,329099	16,201213
44	Vineyard	1,64	41,329068	16,201008
45	Vineyard	2,2	41,329072	16,200355
46	Vineyard	2,51	41,328708	16,199796
47	Vineyard	2,21	41,329219	16,201453
48	Vineyard	2,49	41,283122	16,115112
49	Vineyard	2,53	41,283047	16,114885
51	Vineyard	2,19	41,283349	16,114785
52	Vineyard	1,7	41,283719	16,114794
53	Vineyard	2,1	41,287436	16,124205
54	Vineyard	1,71	41,287559	16,124444

55	Vineyard	2,03	41,287622	16,124522
56	Vineyard	2,13	41,287764	16,125094
57	Vineyard	2,22	41,288	16,1257
58	Vineyard	1,41	41,287661	16,123969
59	Vineyard	1,51	41,288249	16,123341
60	Vineyard	2,14	41,288718	16,123242
61	Vineyard	1,79	41,289174	16,123305
62	Vineyard	1,9	41,290255	16,122861
63	Vineyard	2,36	41,290497	16,12297